Electronic Supplementary Material (ESI) for ChemComm.

Benzothiadiazole-based Pt(II) coordination polymer as efficient heterogeneous photocatalyst for visible-light-driven aerobic oxidative coupling of amines

Shakil Ahmed[a], Atul kumar[a] and Partha Sarathi Mukherjee[a]*

[a]*Department of Inorganic and Physical Chemistry, Indian Institute of Science, Bangalore 560012, India. E-mail: psm@iisc.ac.in*

Materials and methods:

The reagents and solvents used in the current study were obtained from commercial sources and used without further purification. Bruker 400 MHz spectrometer was used to record NMR spectra. PerkinElmer Lambda-750 and Horiba Jobin Yvon Fluoromax4 spectrophotometers were used to record UV/Vis and fluorescence spectra respectively. Transmission Electron Microscopy (TEM) image was obtained by using a ThermoFisher® TecnaiTM T20 – ST instrument operating at 200 kV. Scanning Electron Microscopy (SEM) images and EDS mapping were obtained by using a JEOL SEM IT 300 instrument with the sample deposited on a silicon wafer. Dynamic Light Scattering **(**DLS**)** measurements were performed with a Zetaseizer instrument ZEN3600 **(**Malvern, UK**)** with a 1738 backscattering angle and He-Ne laser (*l*=633 nm).

Synthesis of Acceptor A

50.0 mg of **PI** (38.5 µmol) was taken in a clean 4 mL glass vial. To this vial, 24.7 mg of AgOTf (96.2 µmol) and 0.5 mL of acetone were added. Then the reaction mixture was stirred in dark for 12 hours. Subsequently, the reaction mixture was passed through celite and dried under vacuum to obtain acceptor **A** as a light red solid (60.0 mg). $^{31}P\{^{1}H\}$ NMR (162 MHz, Acetone-d_6): 21.04 (s).

Synthesis of TBP

60.0 mg of the acceptor **A** (44.67µmol) and 13.3 mg of ligand **L** (22.3 µmol) were added into 2 mL DMSO in a 4 mL glass vial. The mixture was stirred at room temperature for 12 h. Subsequently, the mixture was treated with 30 mL of ethyl acetate to produce a reddish-yellow precipitate. The crude product was then washed with 20 mL of diethyl ether thrice. The precipitate was dried under a high vacuum to give a reddish-yellow powder of **TBP** (72.1 mg). ^{1}H NMR (400 MHz, DMSO-d_6): 9.00 (b, 1H), 8.18 (b, 1H), 7.71 (b, 1H), 7.45 (b, 2H), 7.38 – 7.36 (b, 2H), 6.91-6.89 (b, 1H) 2.16 (b, 12H), 1.88 (b, 19H). ^{31}P NMR (162 MHz, DMSO-d_6): 16.77 (s, ^{195}Pt satellites, 1 $J_{Pt\text{-}P}$ = 2204 Hz).

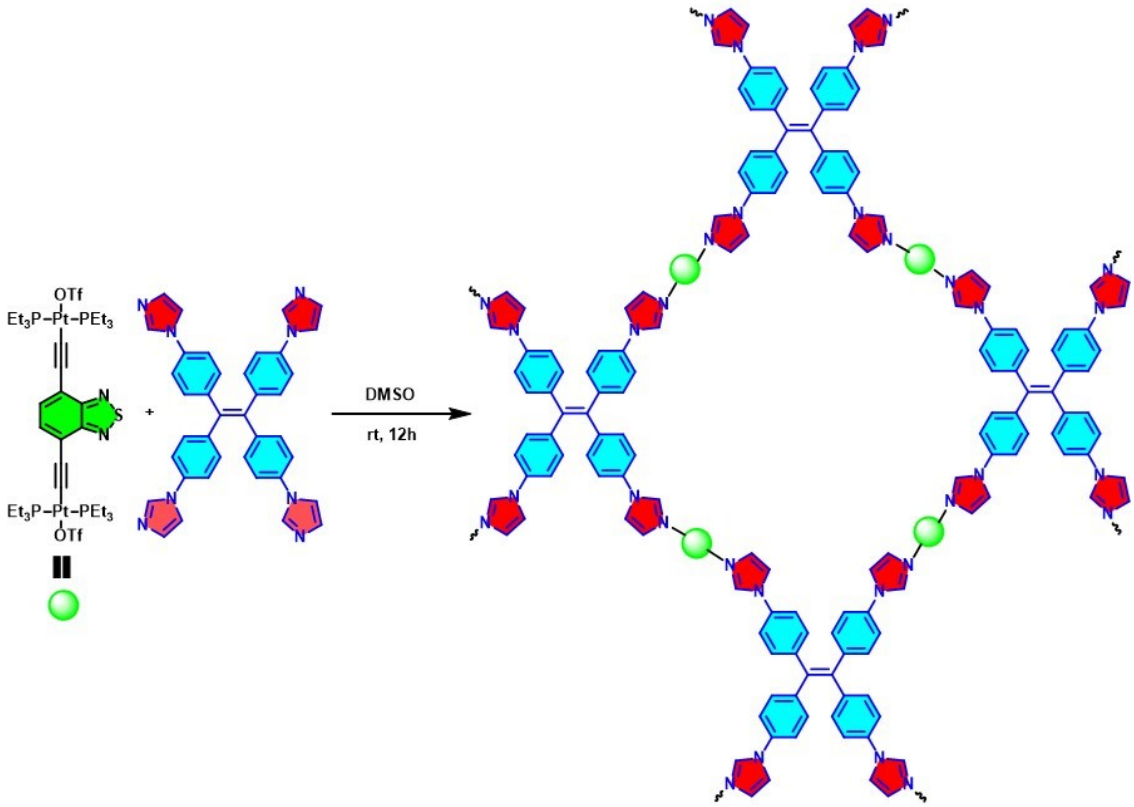

Scheme S1. Schematic representation of the synthesis of **TBP**.

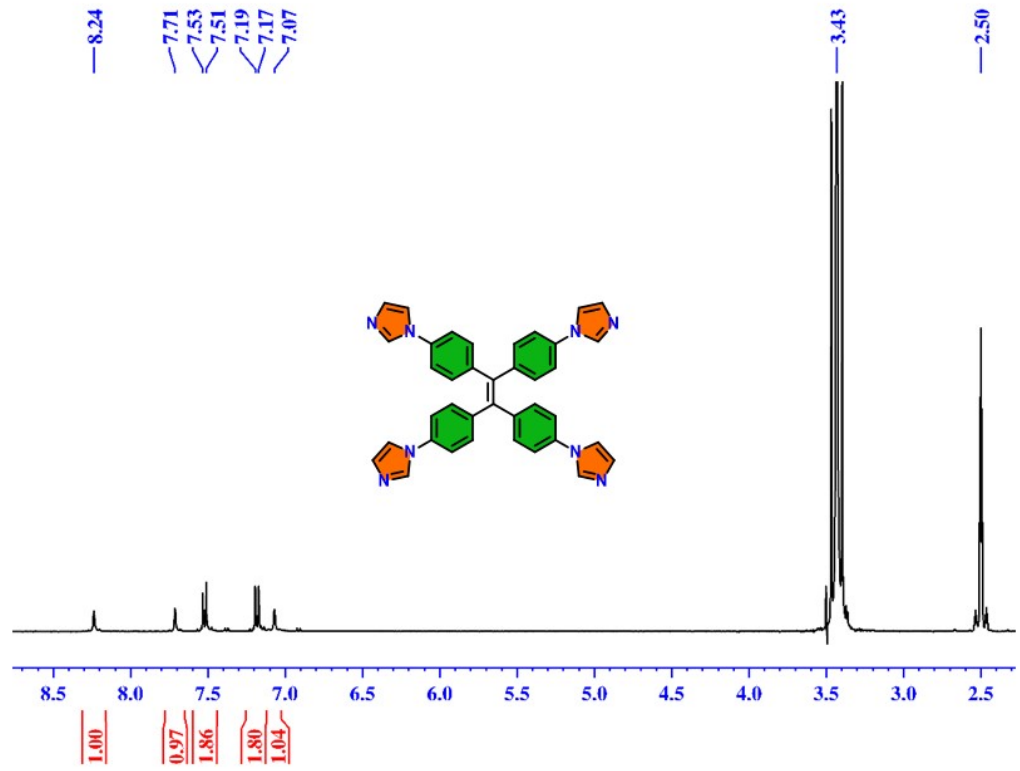

Fig. S1. ^{1}H NMR spectrum of **L** in DMSO-d_6**.**

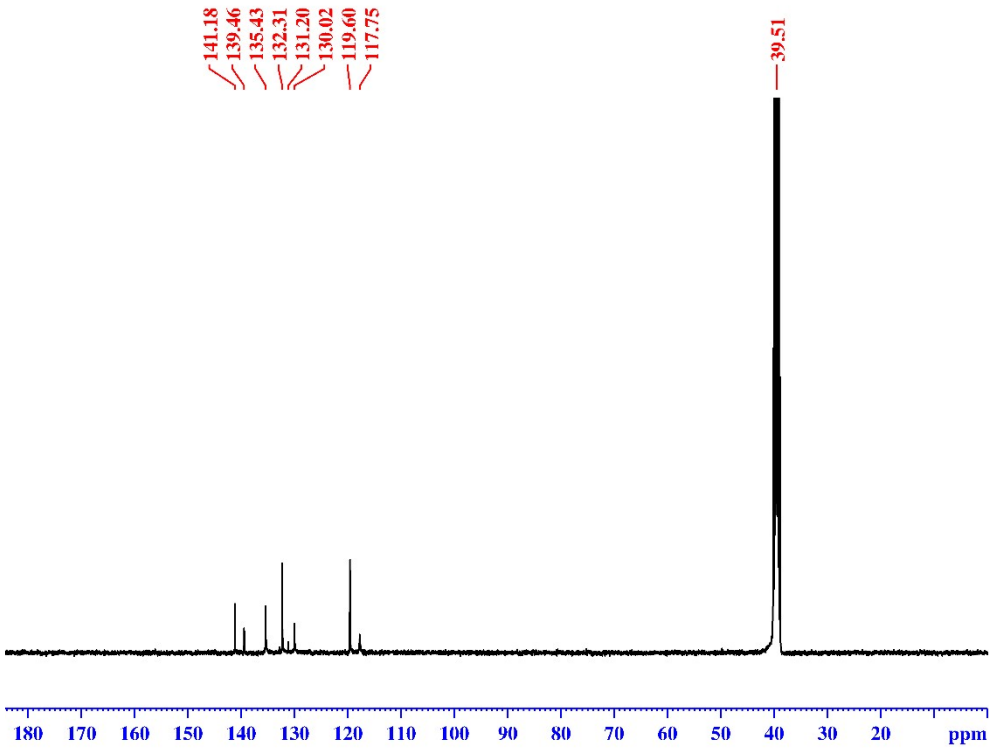

Fig. S2. ^{13}C NMR spectrum of **L** in DMSO-d_6**.**

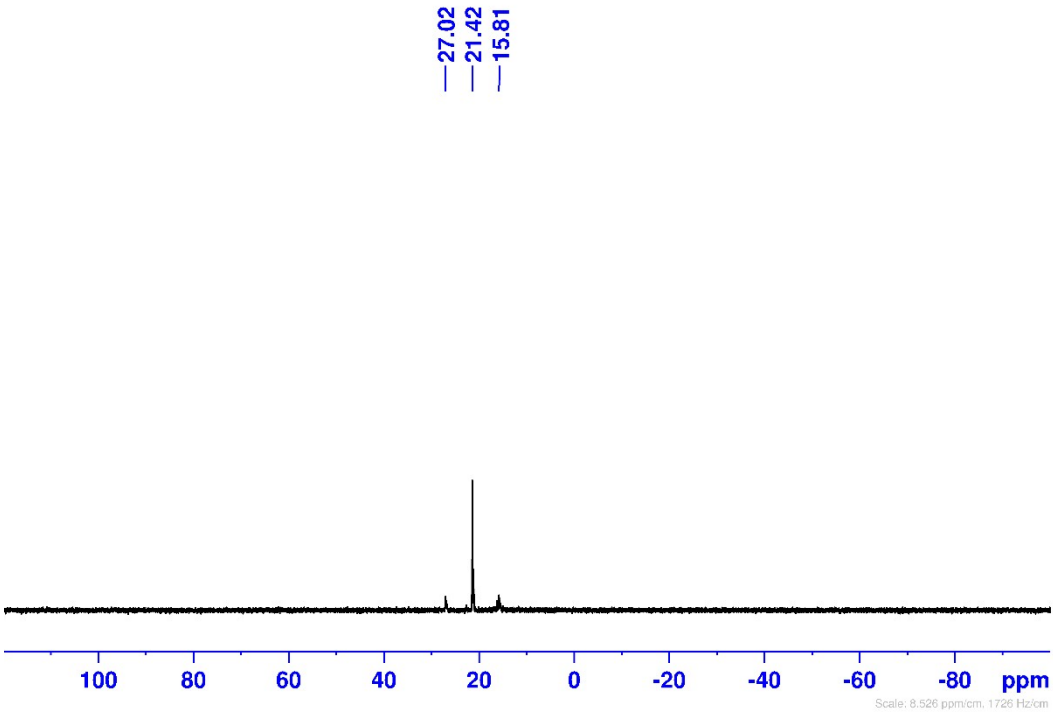

Fig. S3. ^{31}P NMR spectrum of acceptor **A** in acetone-d_6.

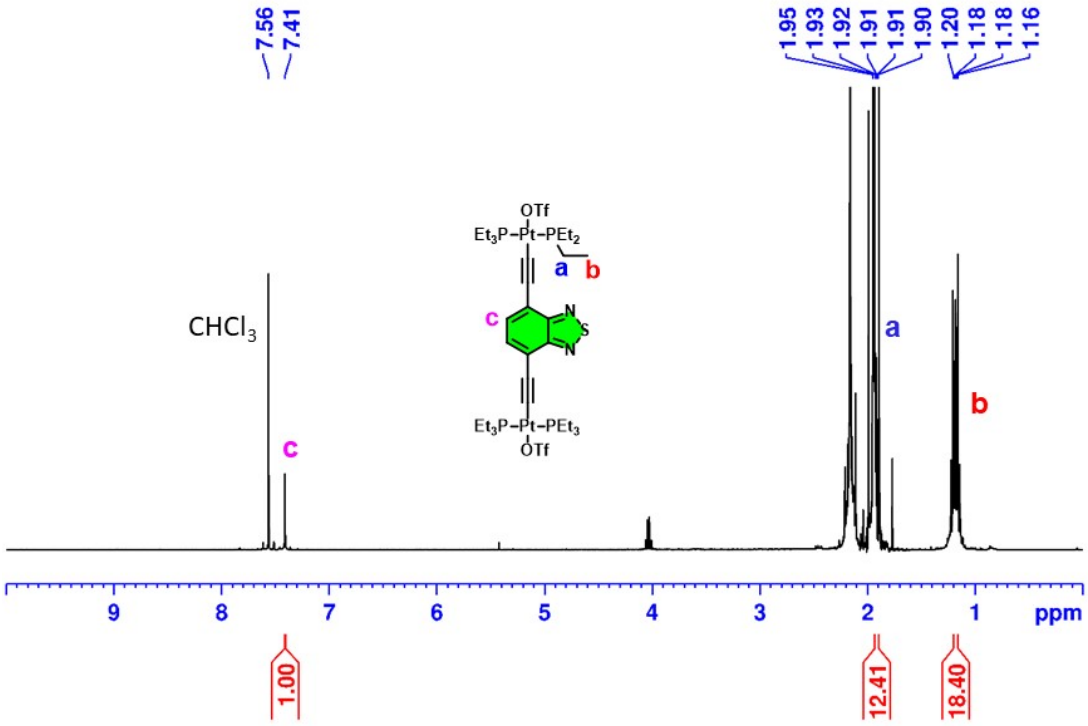

Fig. S4. ^{1}H NMR spectrum of acceptor **A** in Acetonitrile-d_3.

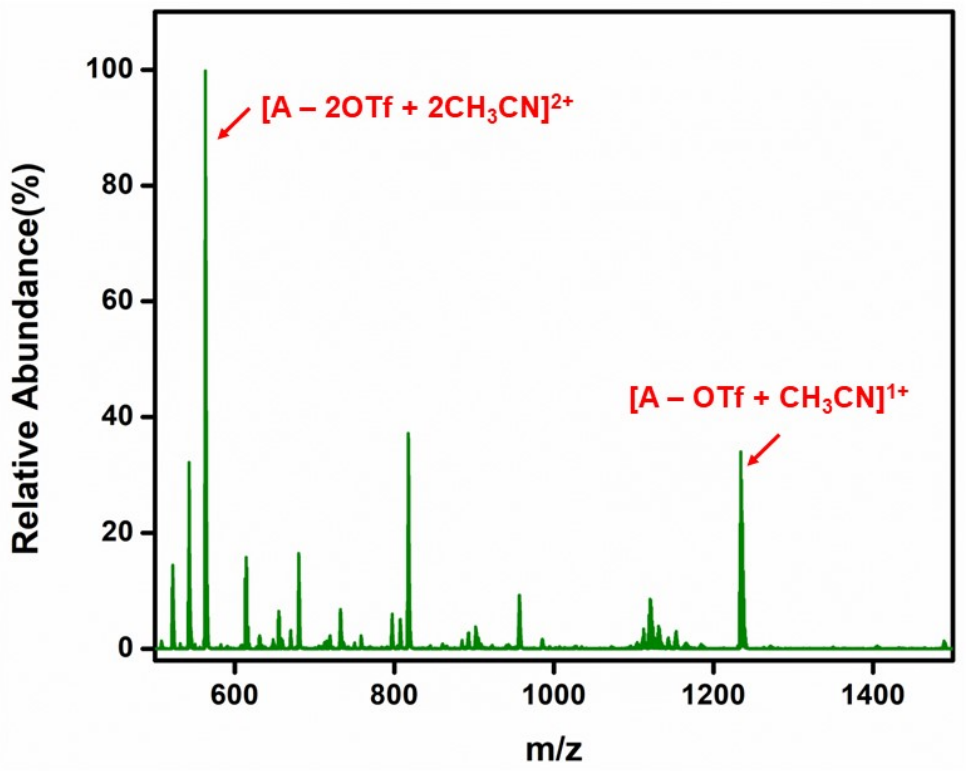

Fig. S5. Mass spectrum of acceptor **A**.

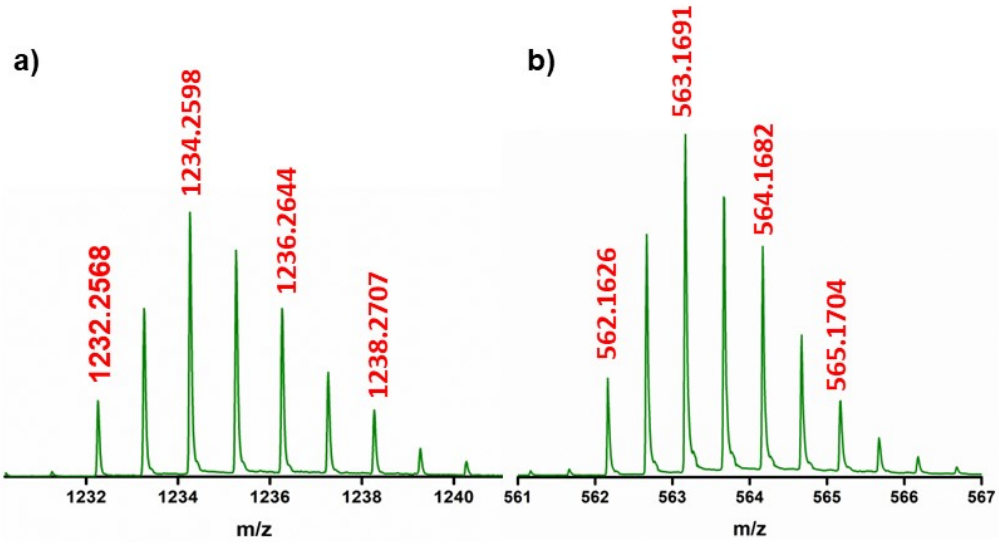

Fig. S6. Isotopic distribution patterns of the peaks corresponding to a) [**A**-OTf+CH_3CN]$^{1+}$, b) [**A**-2OTf+2CH_3CN]$^{2+}$ for acceptor **A**.

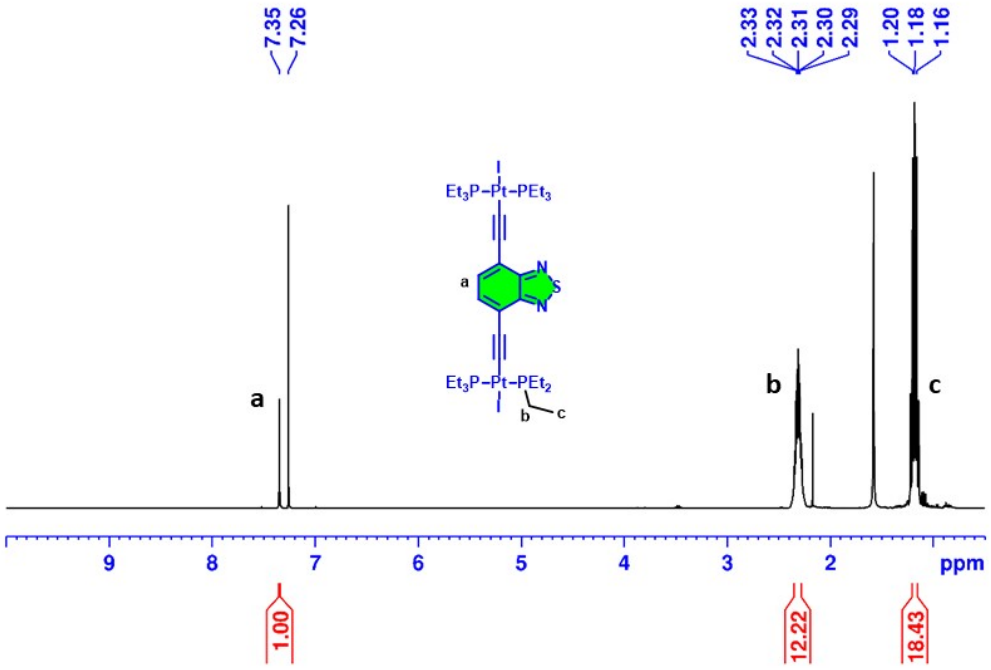

Fig. S7. ^{1}H NMR spectrum of **PI** in $CDCl_3$.

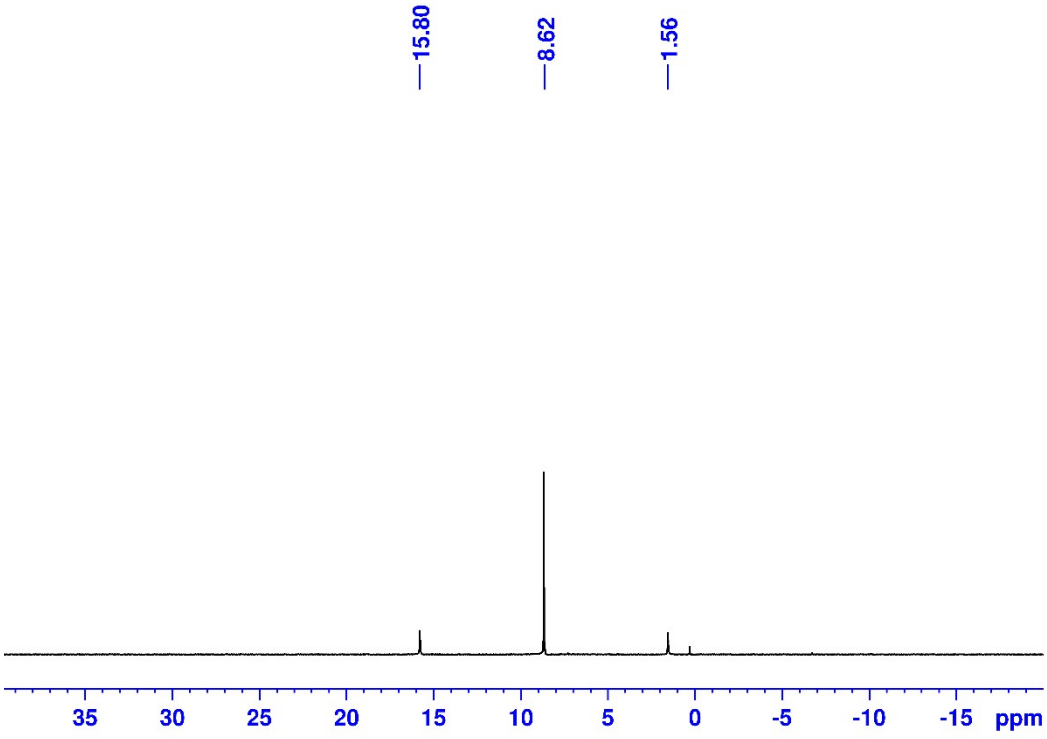

Fig. S8. ^{31}P NMR spectrum of **PI** in $CDCl_3$.

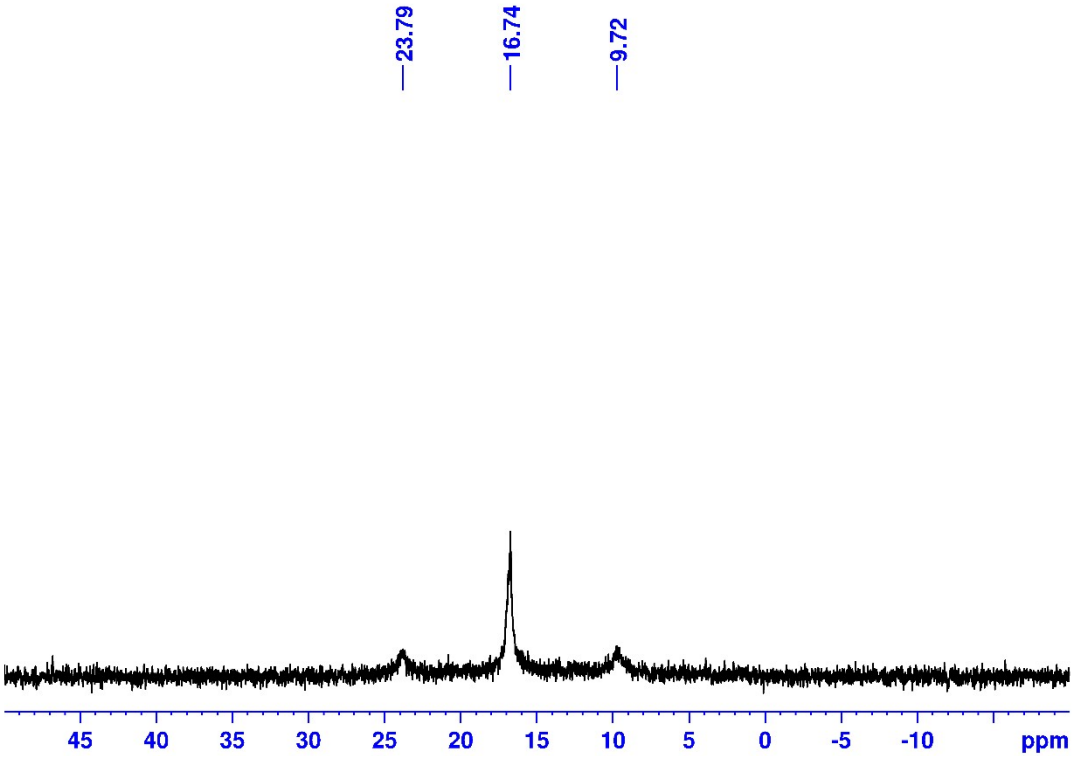

Fig. S9. ^{31}P NMR spectrum of **TBP** in DMSO-d_6**.**

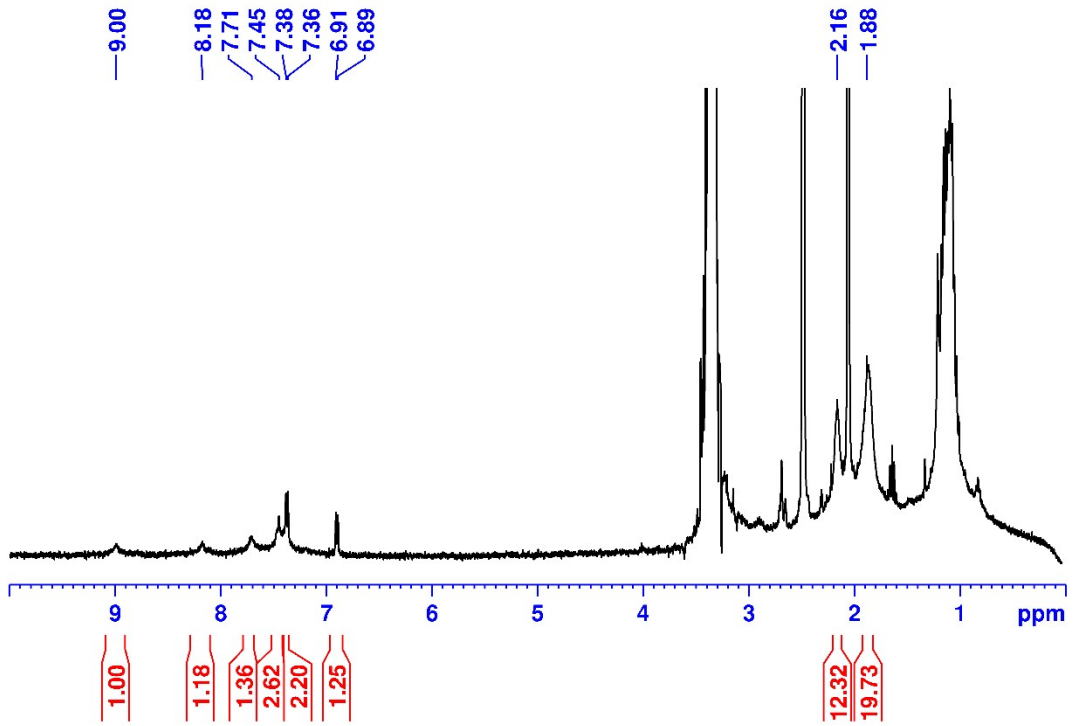

Fig. S10. ^{1}H NMR spectrum of **TBP** in DMSO-d_6**.**

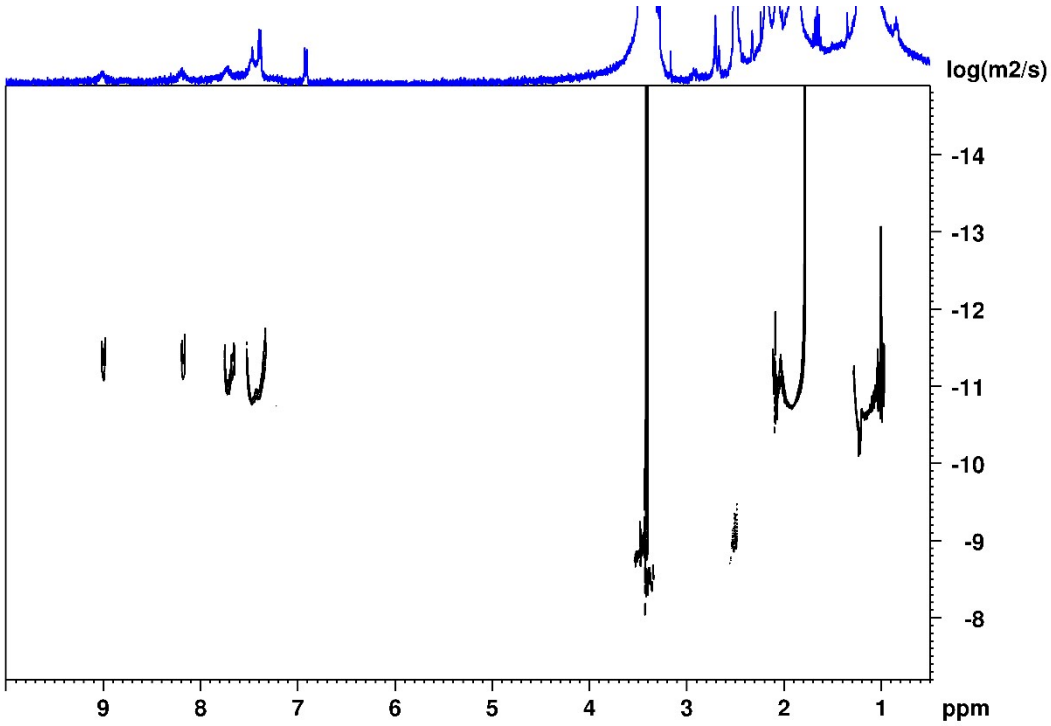

Fig. S11. DOSY NMR of the polymer **TBP** in DMSO-d_6**.**

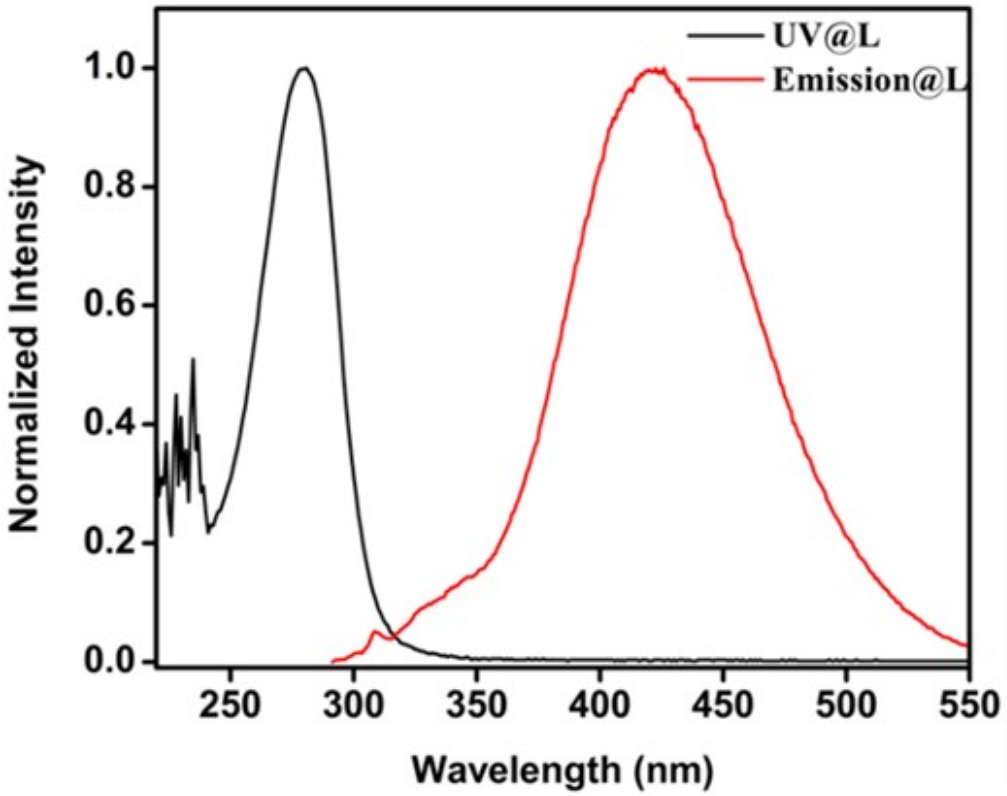

Fig. S12. Normalized UV-Vis and emission spectra in DMSO for **L**.

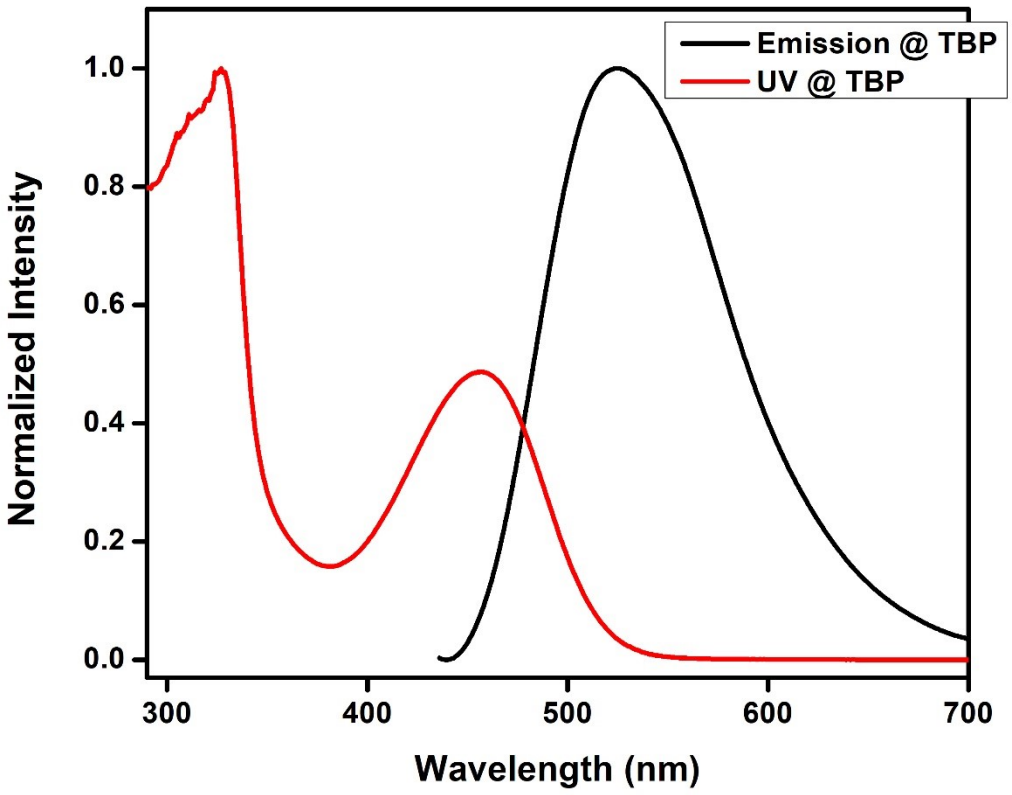

Fig. S13. Normalized UV-Vis and emission spectra in DMSO for **TBP**.

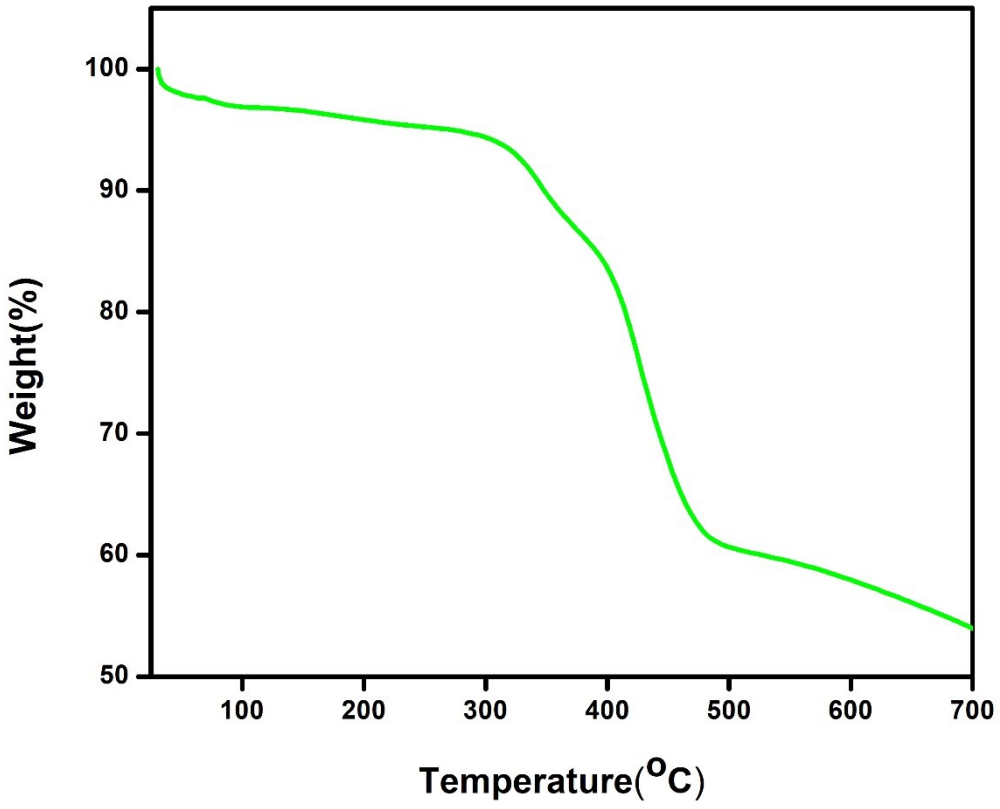

Fig. S14. TGA of polymer **TBP**.

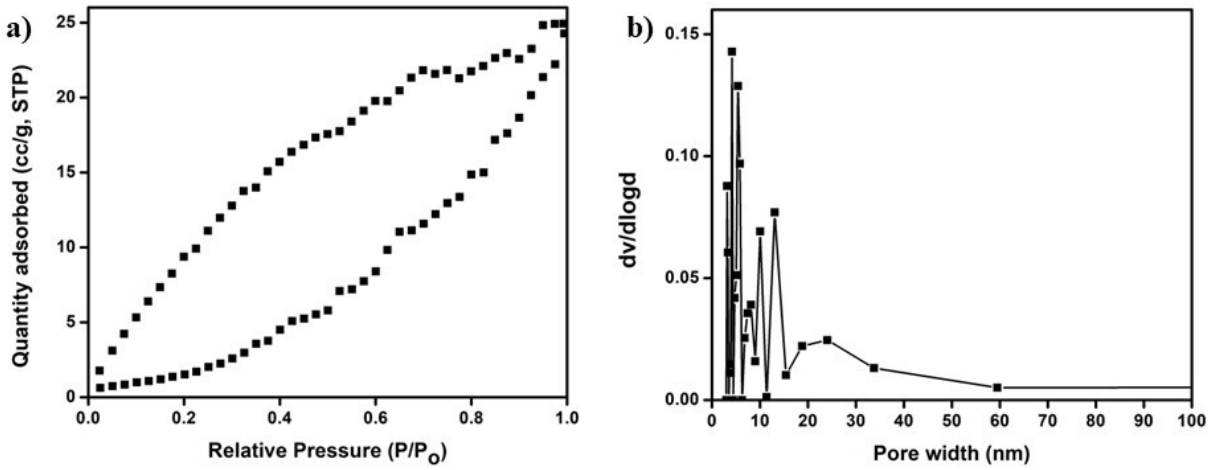

Fig. S15. a) N_2 adsorption-desorption isotherms; b) pore size distribution profile of **TBP** at 77K.

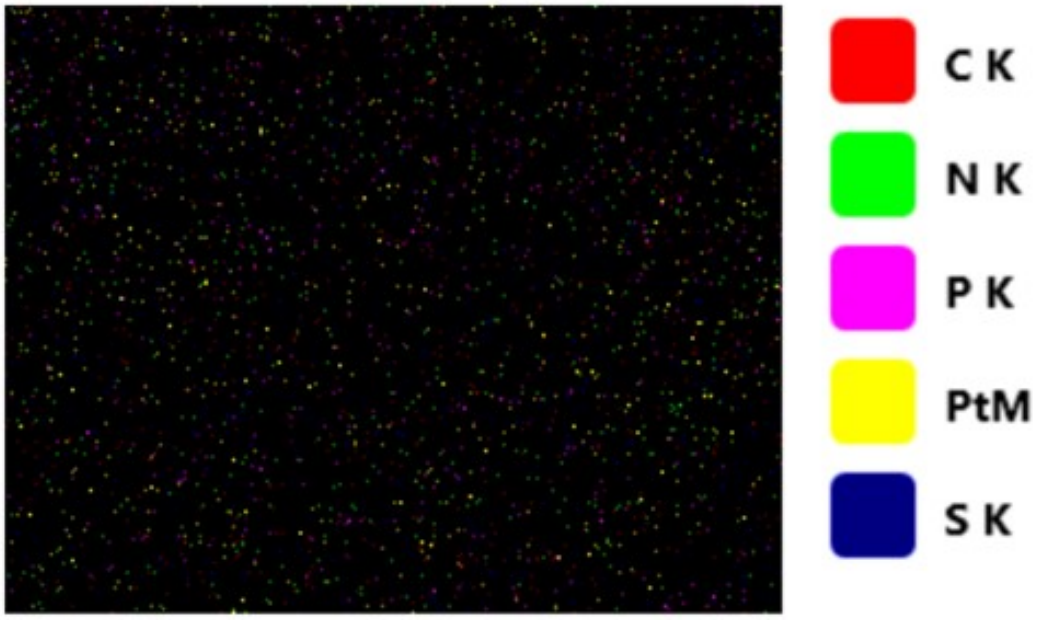

Fig. S16. EDS mapping of **TBP**.

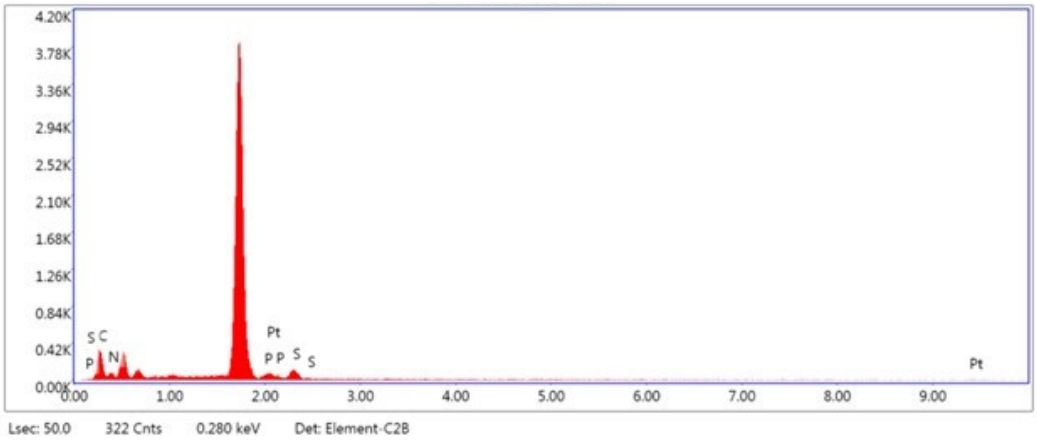

Fig. S17. EDS analysis of **TBP**.

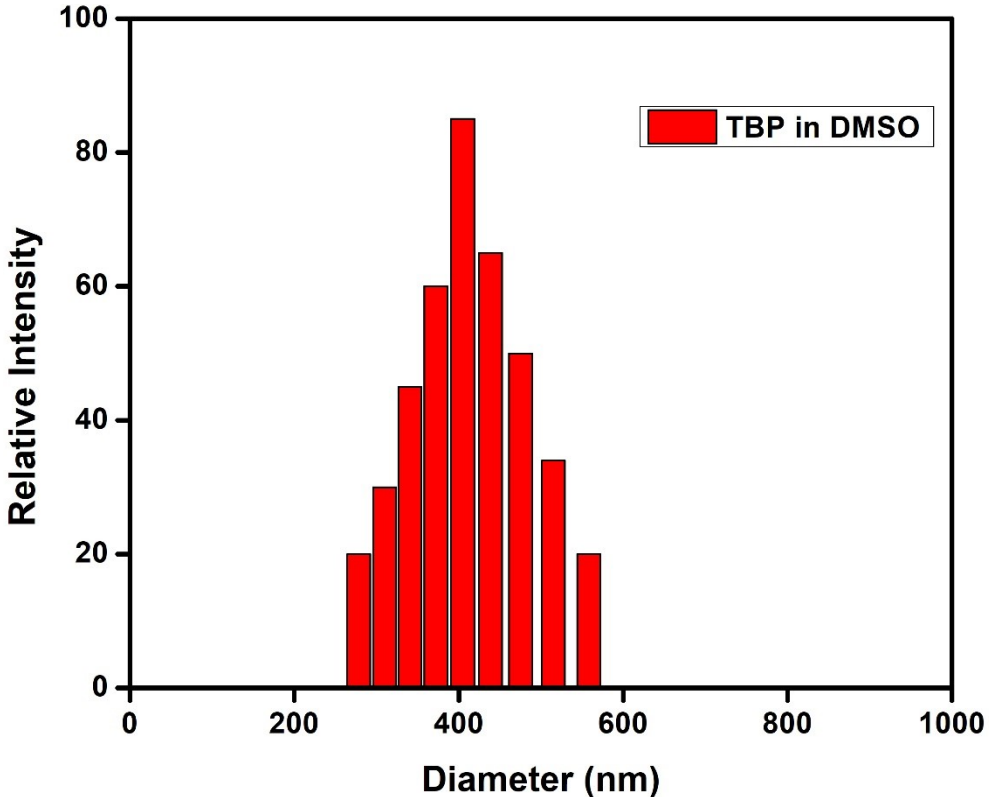

Fig. S18. DLS data for **TBP**.

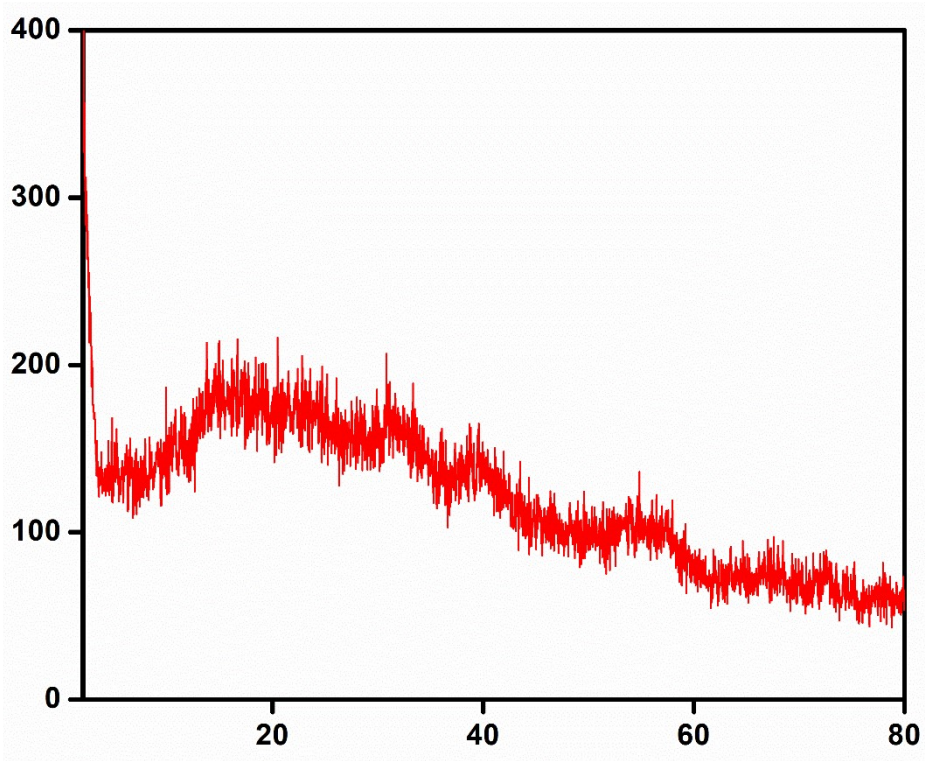

Fig. S19. PXRD of **TBP**.

Scheme S2: Visible-light-driven oxidative coupling of various primary benzylamines.

NMR spectra of the reaction mixtures with various substituents on the benzylamines after 2 hours are given below (Figs. S18-32).

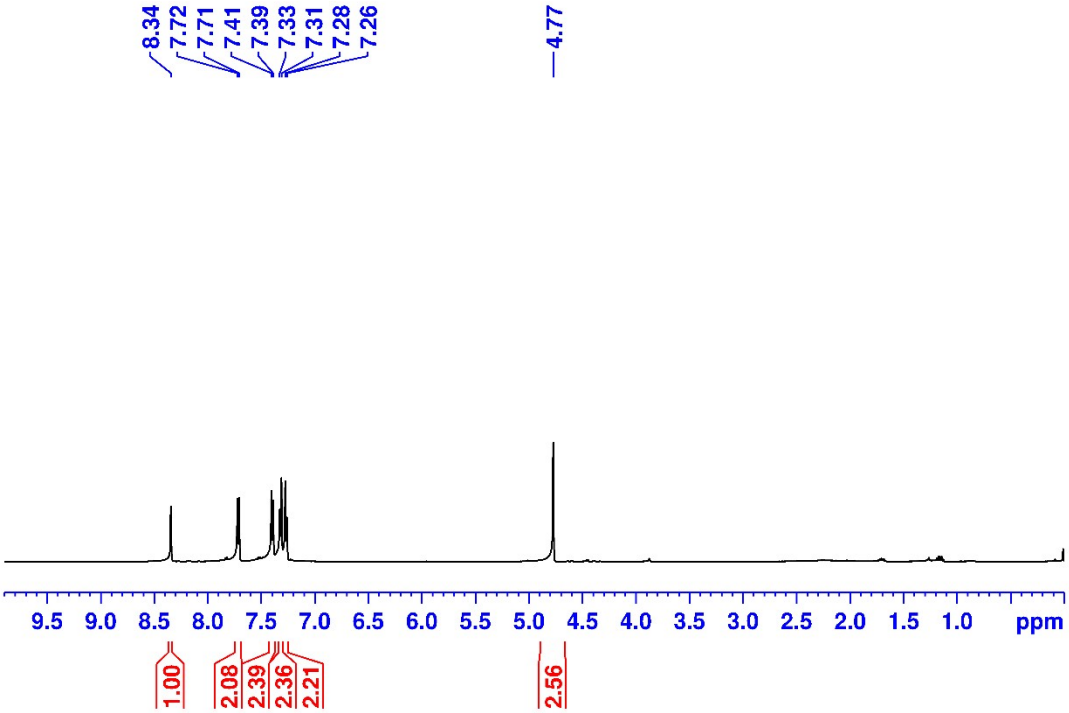

Fig. S20. ^{1}H NMR of (**R = 4-Cl**) in $CDCl_3$.

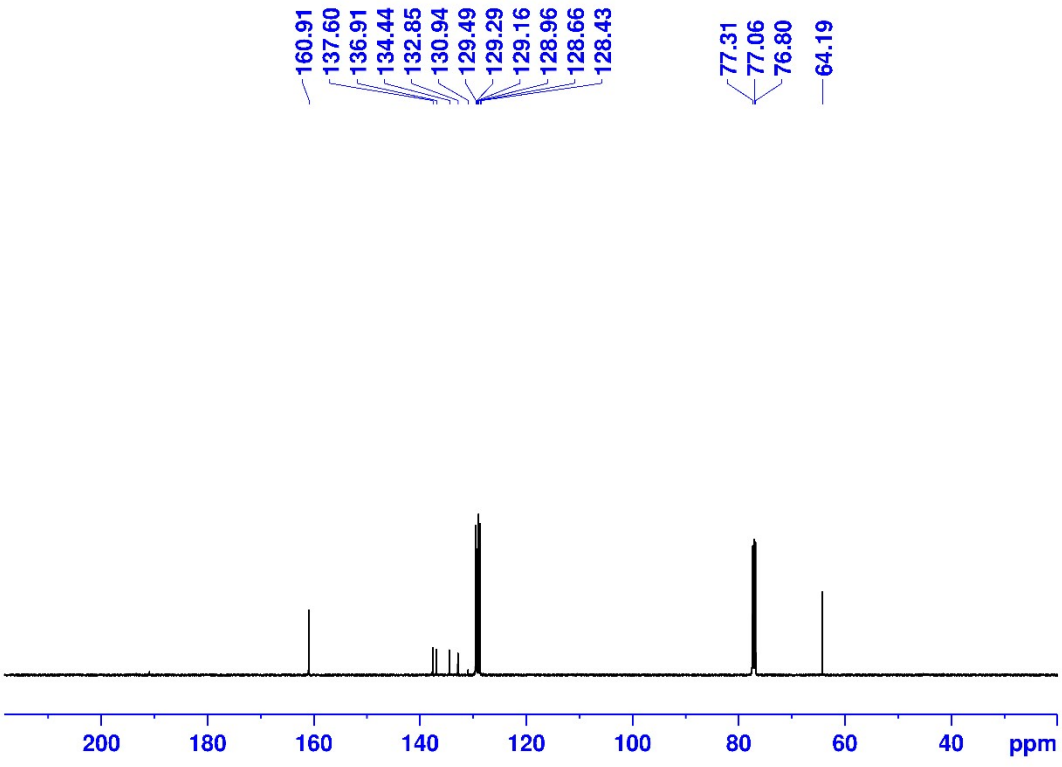

Fig. S21. ^{13}C NMR of (**R = 4-Cl**) in $CDCl_3$.

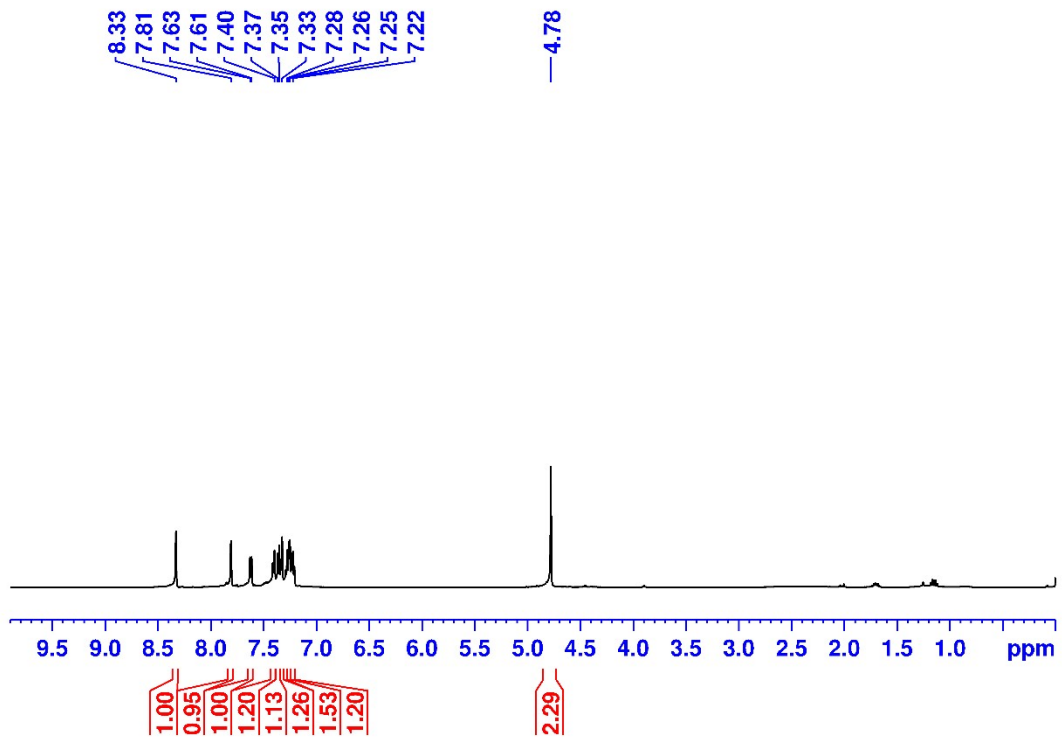

Fig. S22. ^{1}H NMR of (**R = 3-Cl**) in $CDCl_3$.

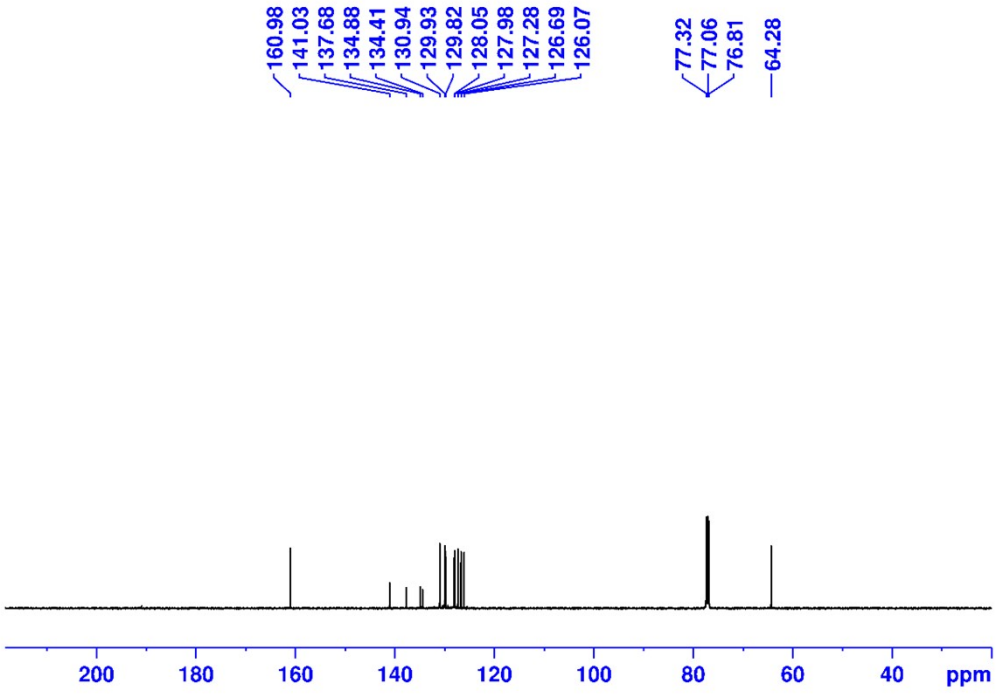

Fig. S23. ^{13}C NMR of (**R = 3-Cl**) in $CDCl_3$.

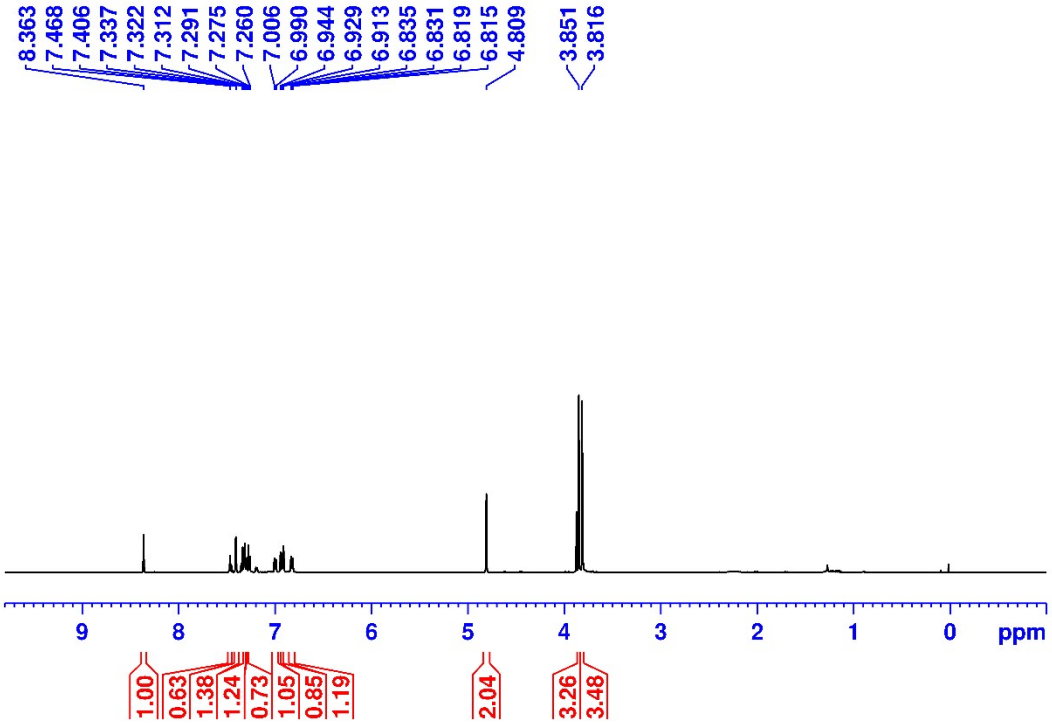

Fig. S24. ^{1}H NMR of (**R = 3-OMe**) in $CDCl_3$ {m/z = 256.1304 (experimental), 256.1337

(theoretical)}.

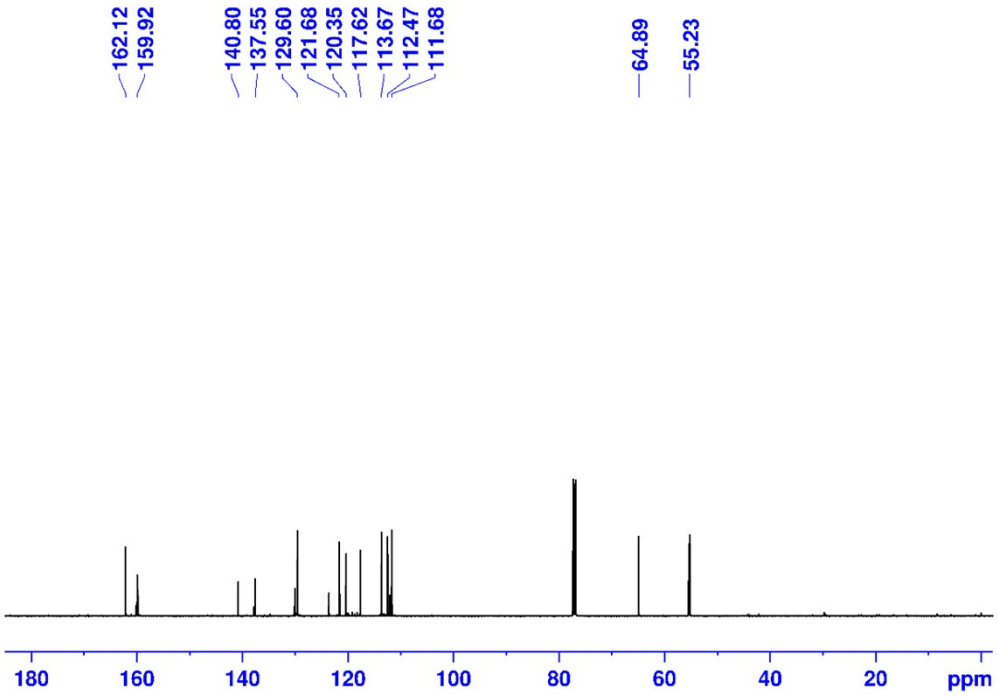

Fig. S25. ^{13}C NMR of (**R = 3-OMe**) in $CDCl_3$.

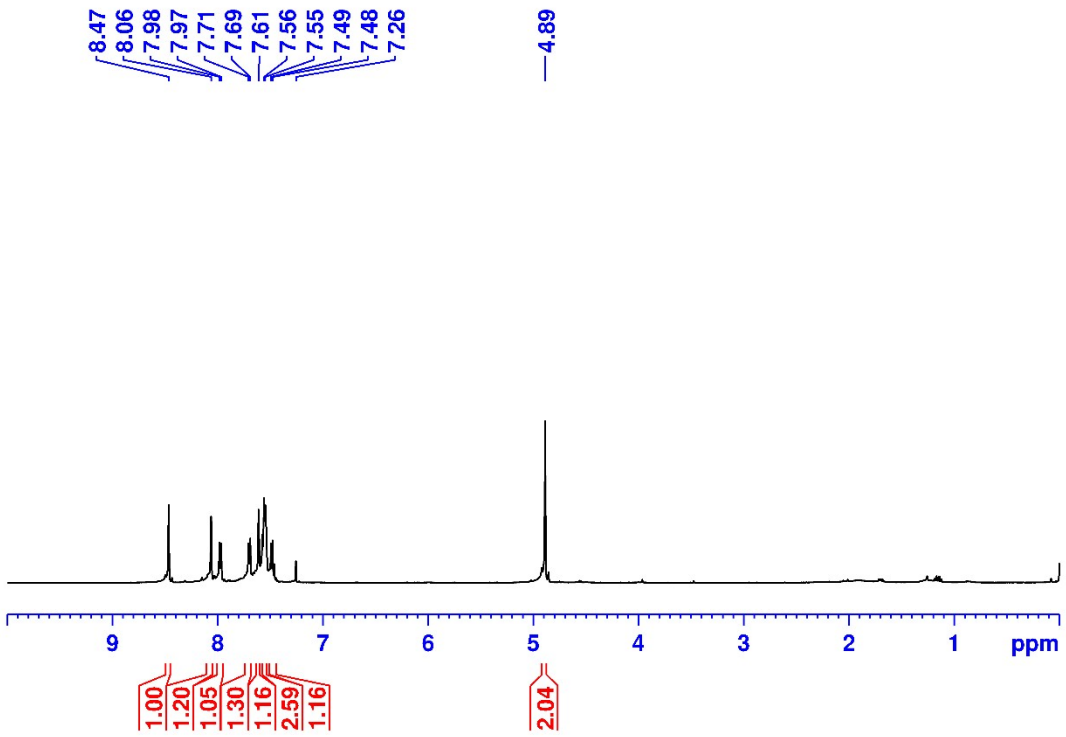

Fig. S26. ^{1}H NMR of (**R = 3-CF_3**) in $CDCl_3$.

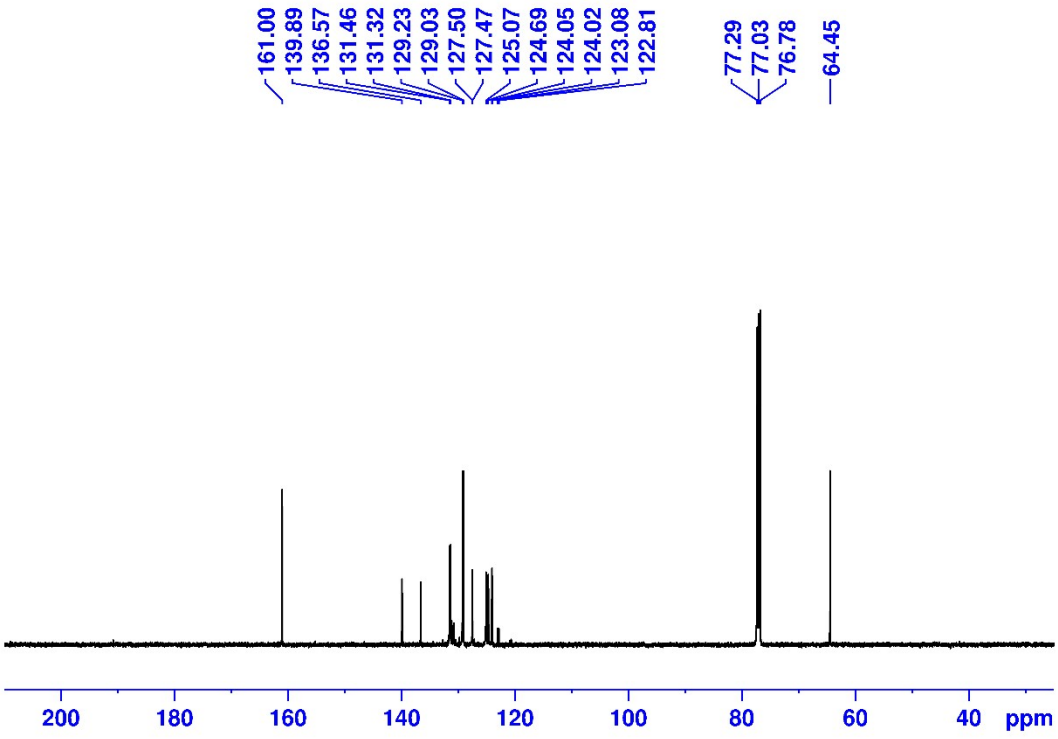

Fig. S27. ^{13}C NMR of (**R = 3-CF_3**) in $CDCl_3$.

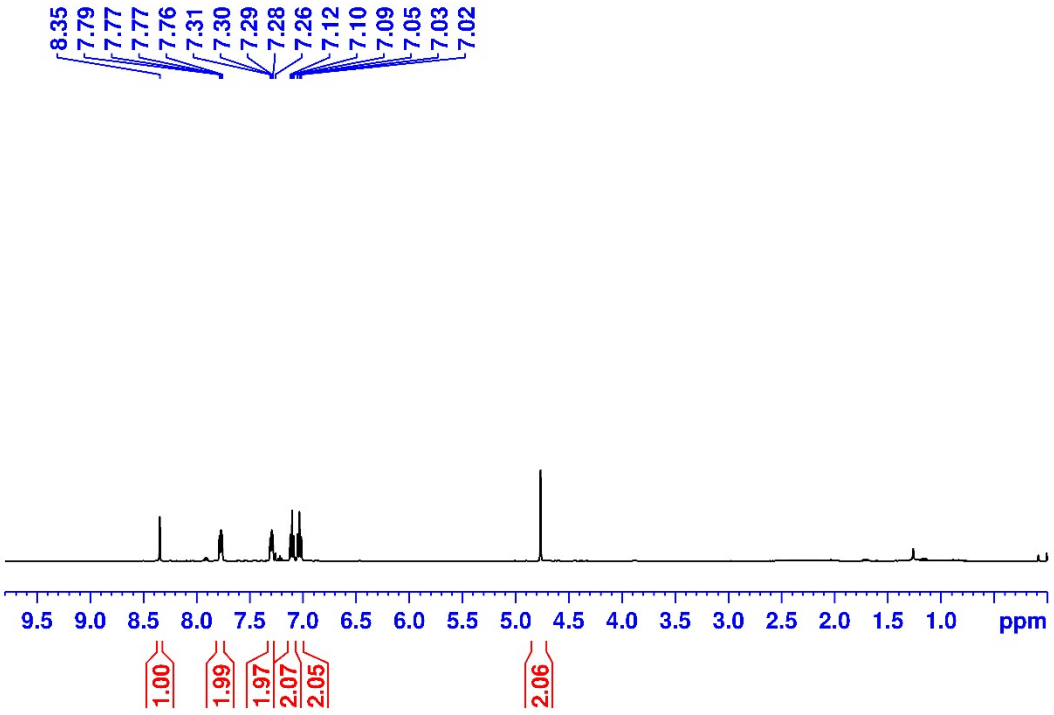

Fig. S28. ^{1}H NMR of (**R = 4-F**) in $CDCl_3$.

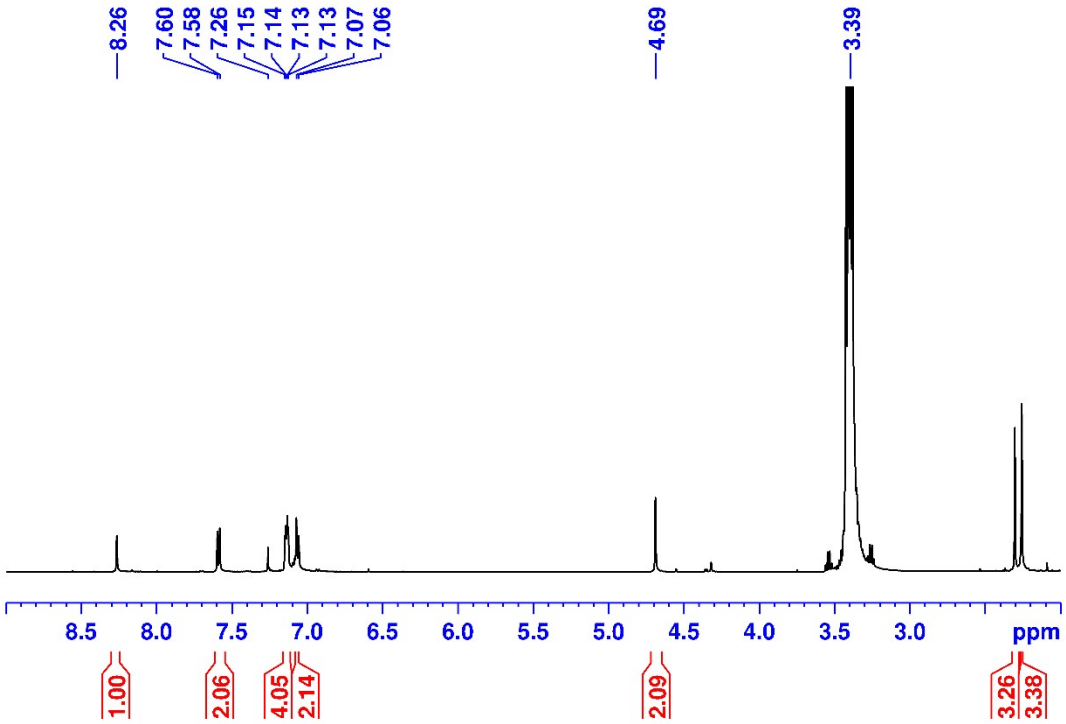

Fig. S29. ^{1}H NMR of (**R = 4-CH_3**) in $CDCl_3$ {m/z = 224.1394 (experimental), 224.1439 (theoretical)}.

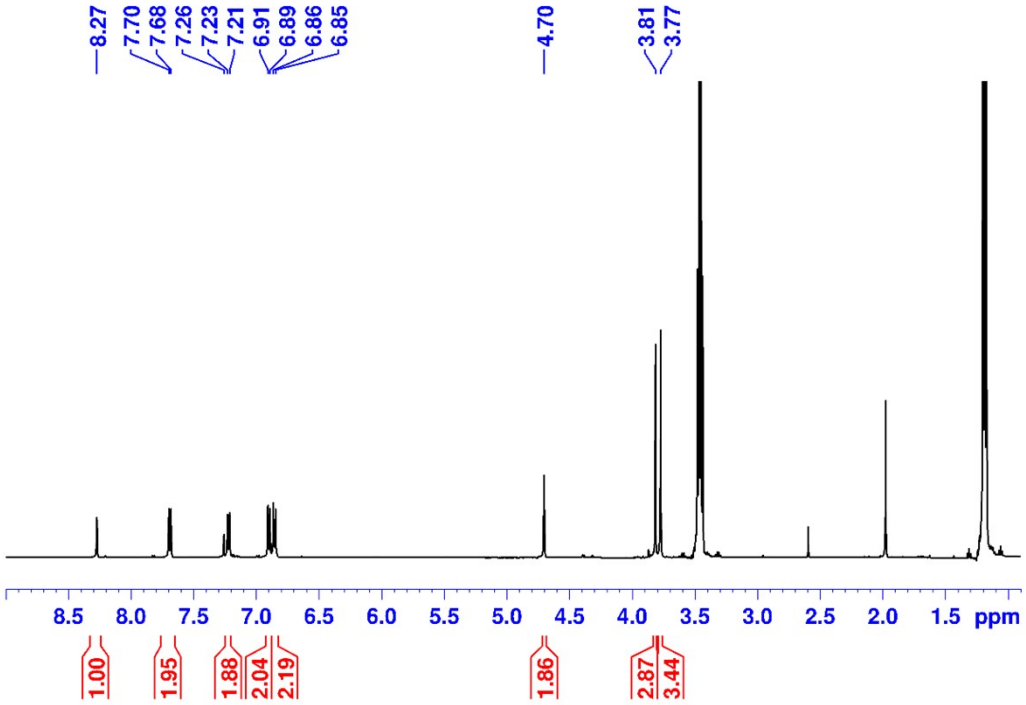

Fig. S30. ^{1}H NMR of (**R = 4-OMe**) in $CDCl_3$. {m/z = 256.1304 (experimental), 256.1337 (theoretical)}.

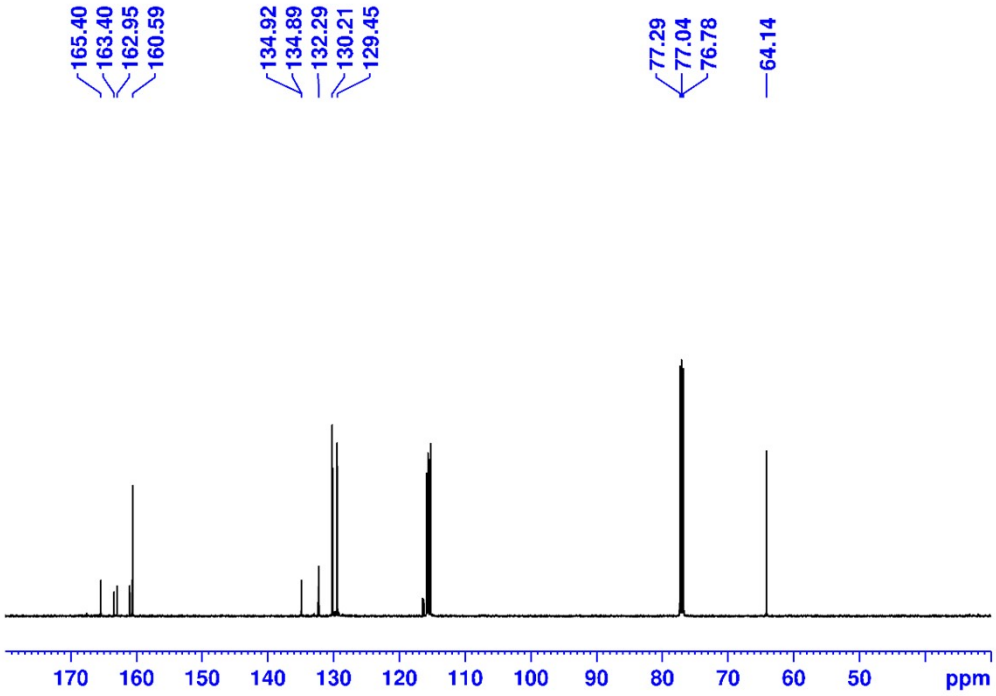

Fig. S31. ^{13}C NMR of (**R = 4-OMe**) in $CDCl_3$.

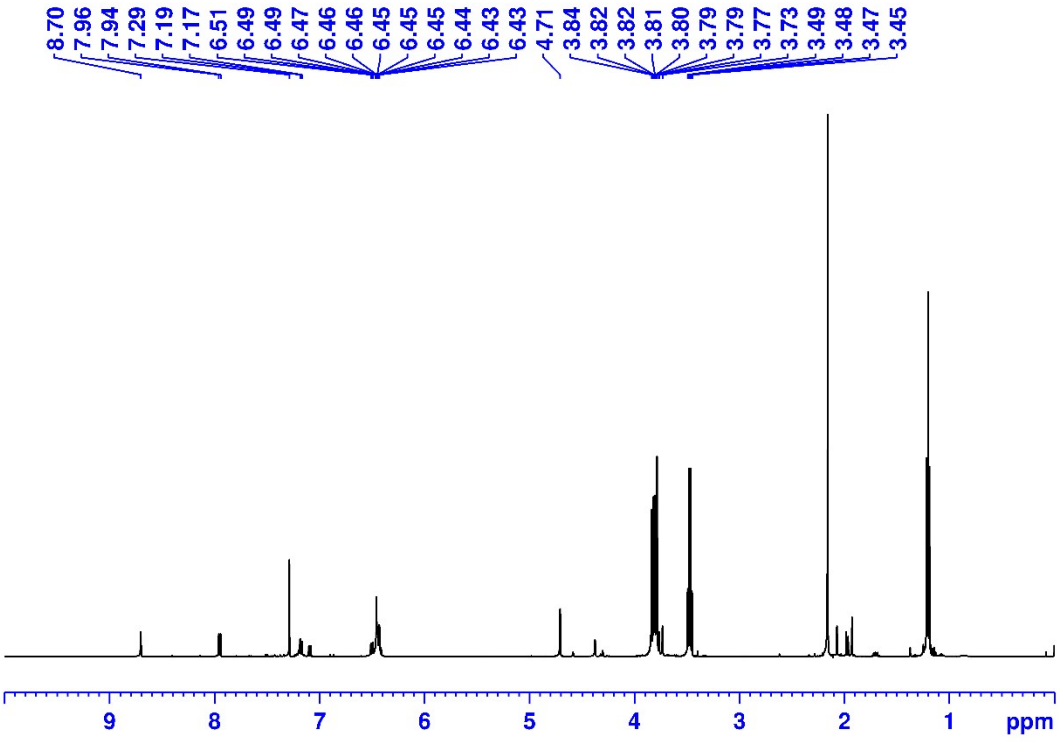

Fig. S32. ^{1}H NMR of (**R = 2, 4-OMe**) in $CDCl_3$ {m/z = 316.1508 (experimental), 316.1549 (theoretical)}.

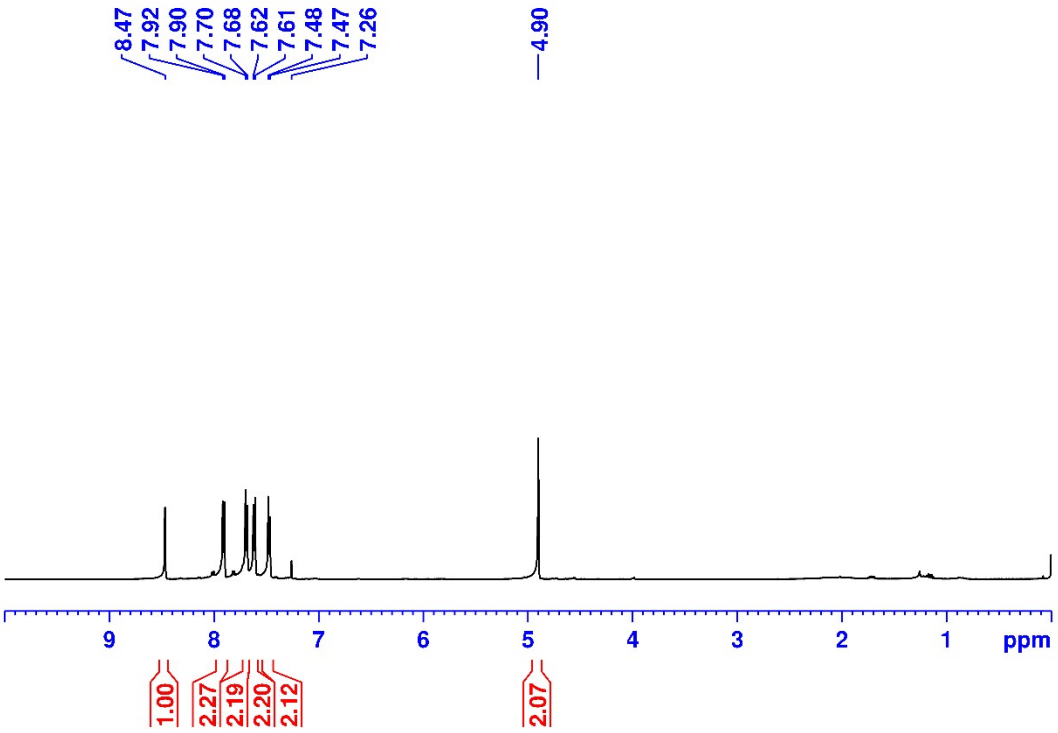

Fig. S33. ^{1}H NMR of (**R = 4-CF_3**) in $CDCl_3$.

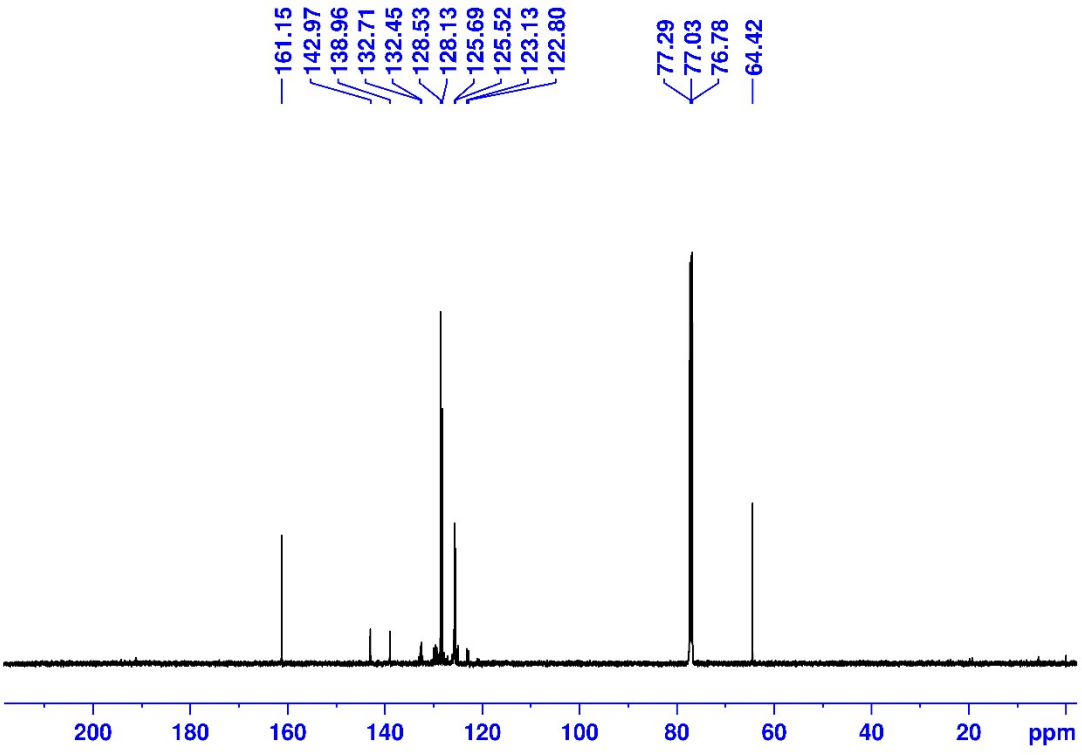

Fig. S34. ^{13}C NMR of (**R = 4-CF_3**) in $CDCl_3$.

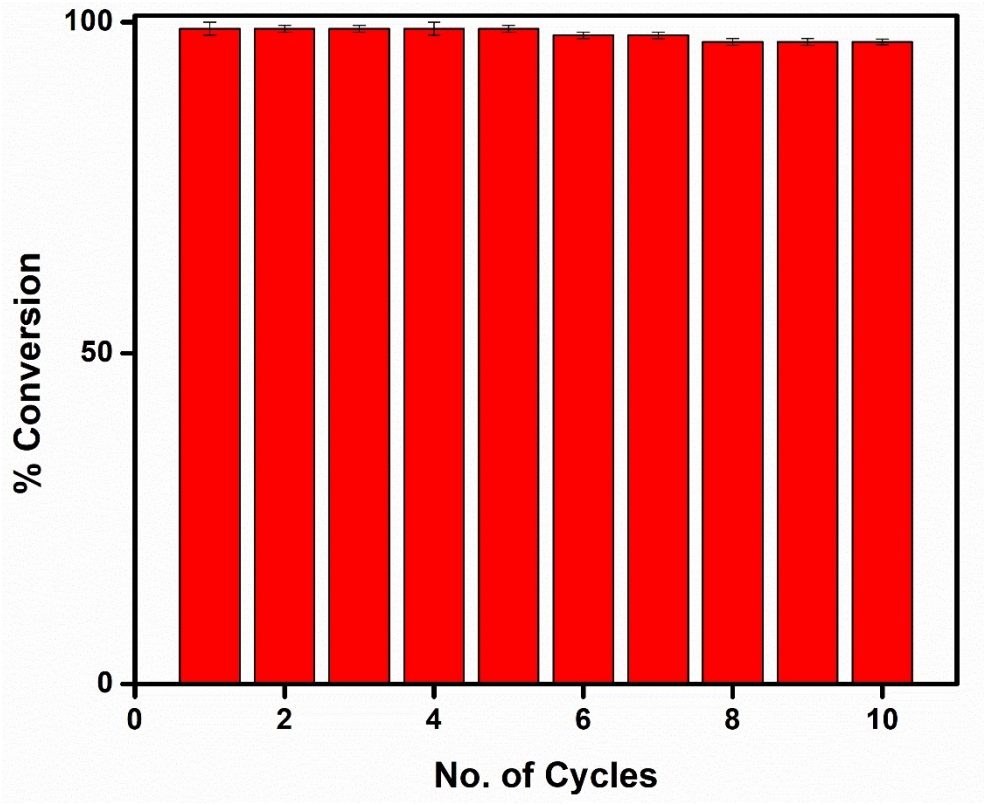

Fig. S35. Recyclability of **TBP** as photocatalyst for the reaction of 4-methylbenzylamine (**R** = 4-CH_3).

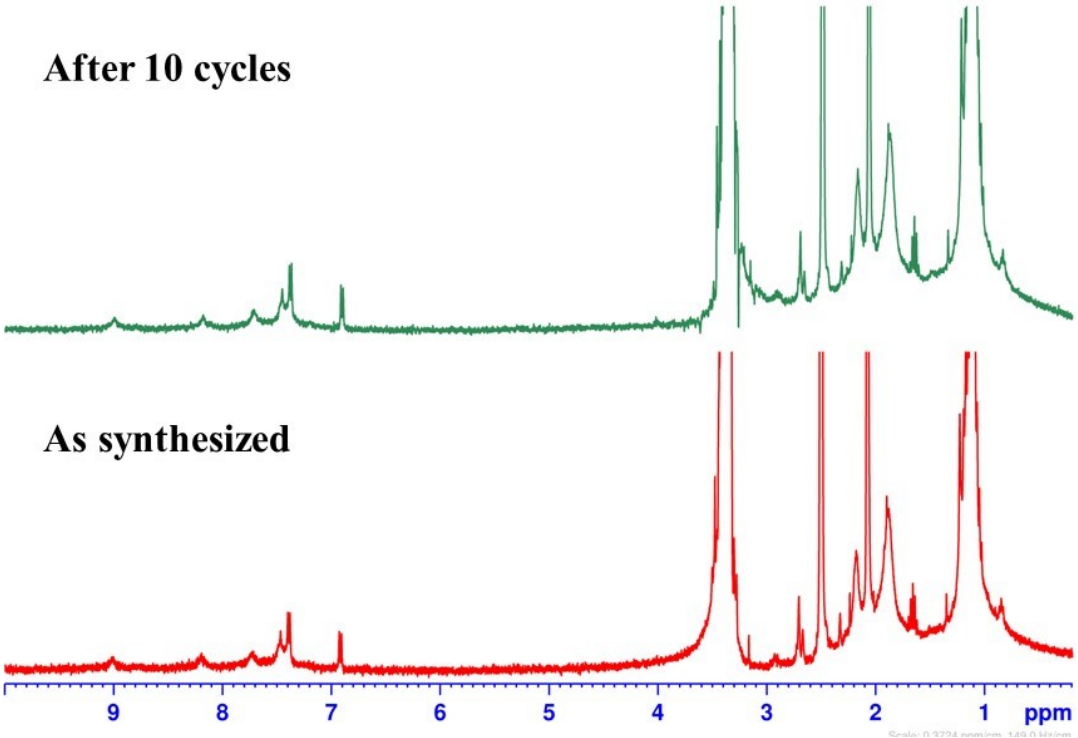

Fig. S36. ^{1}H NMR spectra of **TBP** as synthesized (below) and after 10 cycles (above) of use for the reaction of 4-methylabenzylamine. A similar NMR pattern was also observed for the

recovered catalyst after 10 cycles of use for the conversion of other substituted benzylamines to their corresponding imines.

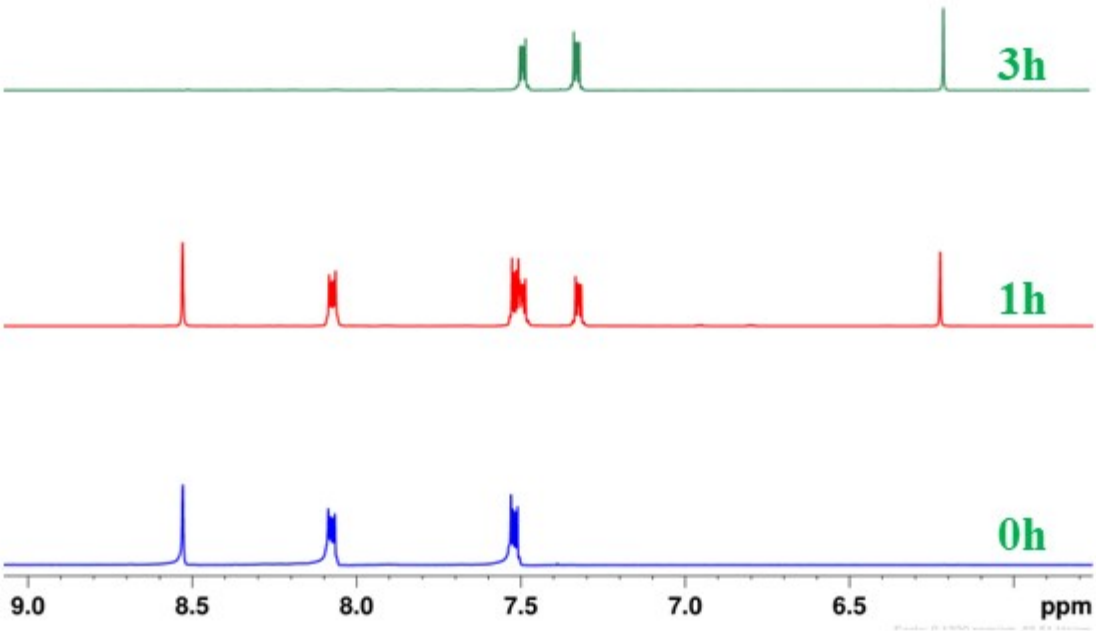

Fig. S37. Time-dependent ^{1}H NMR of anthracene upon visible light irradiation (λ > 400 nm) in the presence of **TBP**.

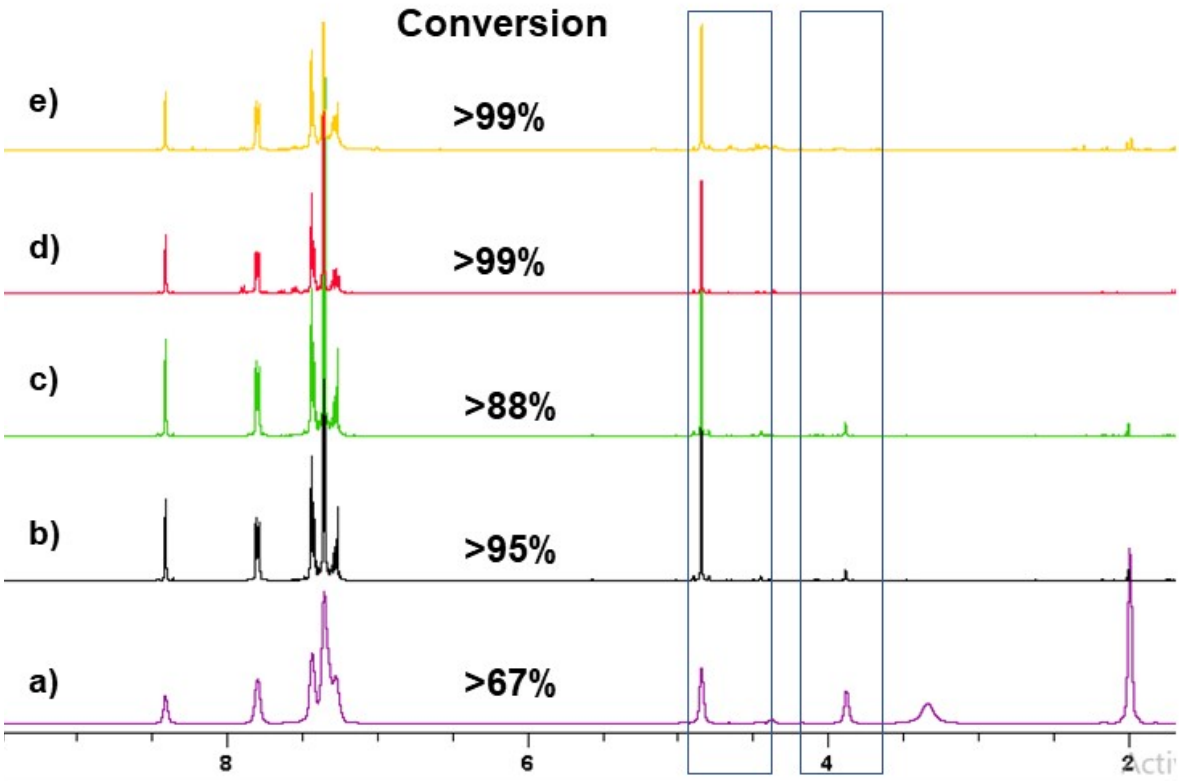

Fig. S38. ^{1}H NMR of the reaction mixture of oxidative coupling of benzylamine using **TBP** as photocatalyst a) after 1 hr (1.0 atm O_2, 0.5 mL acetonitrile), b) without CH_3CN (1.0 atm O_2), c)

in presence of 0.5 mmol benzoquinone (1.0 atm O_2, 0.5 mL acetonitrile), d) after 8 h (air, 0.5 mL acetonitrile), and e) after 2 h (1.0 atm O_2, 0.5 mL acetonitrile).

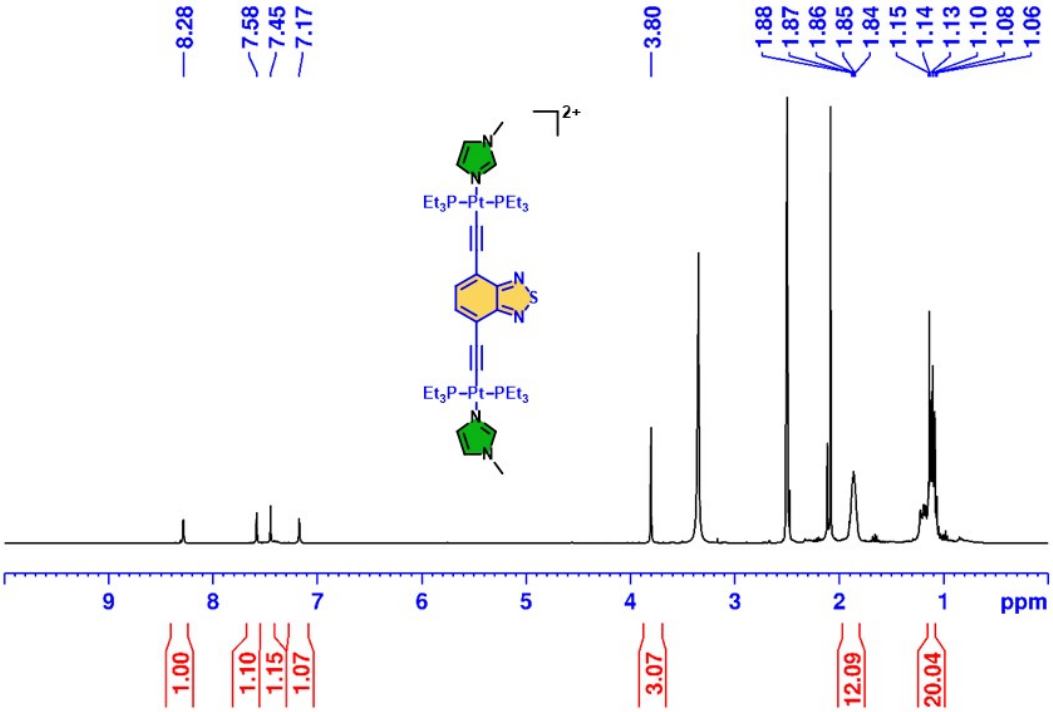

Fig. S39. ^{1}H NMR of the model complex **M** in DMSO-d_6.

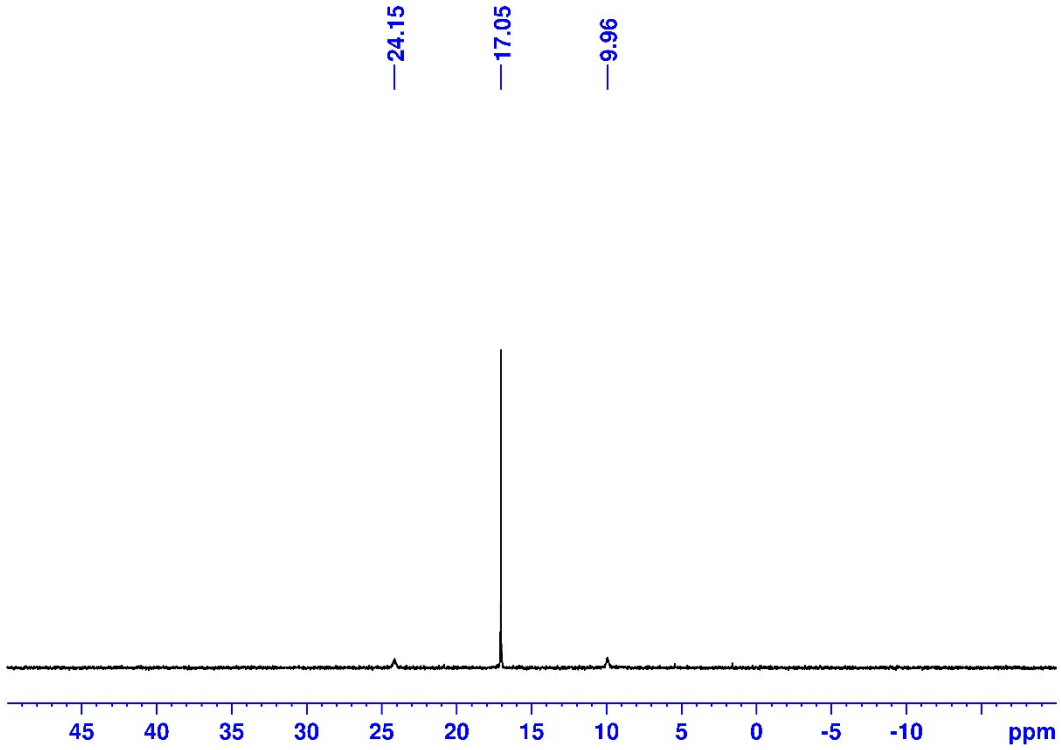

Fig. S40. ^{31}P NMR of the model complex **M** in DMSO-d_6.

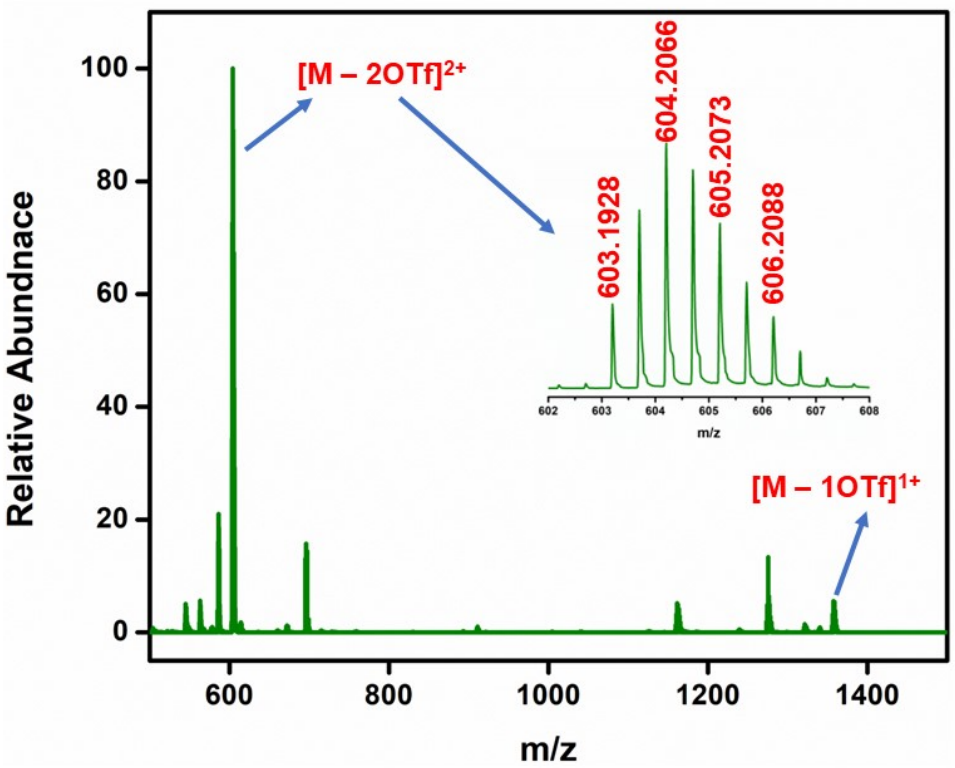

Fig. S41. Mass spectrum of the model complex **M**.

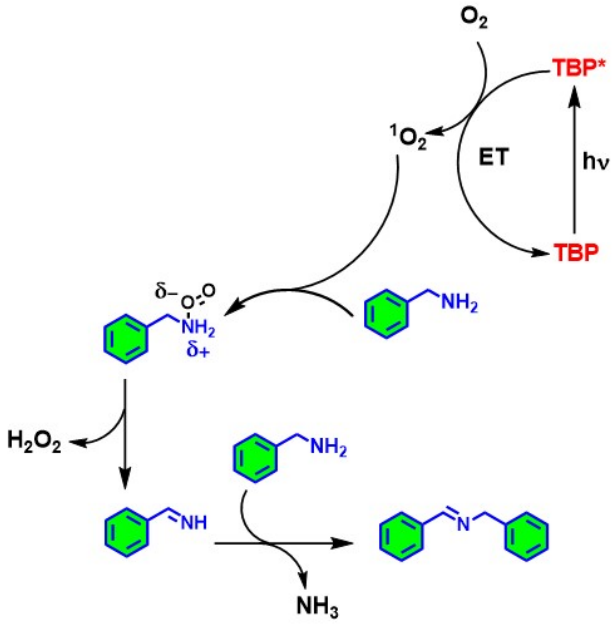

Scheme S2. Plausible reaction mechanism of the visible-light-driven aerobic oxidative coupling reaction of amines catalyzed by **TBP**.

Plausible Mechanism: In the catalytic pathway, the excited state of **TBP** (**TBP***) transfers energy to O_2 molecules under visible light irradiation, leading to the formation of $^1O_2$. $^1O_2$ subsequently captures two protons from benzylamine. As a result, H_2O_2 and Ph-CH=NH are formed from benzylamine. Subsequently, N-benzylidenebenzylamine is further generated as a final product by the nucleophilic addition reaction of Ph-CH=NH and benzylamine.

Table S1. Comparison of photocatalytic performance with previously reported photocatalysts.

Entry	Catalyst	Light Source	Time	Oxidant	Temperature (^{0}C)	Yield (%)	Reference
1	TBP	45 W white LED	2h	O_2	RT	99%	This work
2	ZnW–PYI	10W white LED lamp	36h	air	RT	92	1
3	ZnW–DPNDI–PYI	10W white LED lamp	16h	air	RT	99	2
4	BTDA-TAPT	300 W Xe lamp (λ > 420 nm)	3h	O_2	30	97	3
5	2H WSe2	45 W white LED	48h	O_2	50	95	4
6	Ag_3PO_4	solar simulator	40 min	air	RT	95	5
7	ZJU-56-0.2	660 nm NIR LEDs	24 h	O_2	60	62	6
8	ZnO(0.1)@g CN-UA/MA	Xe lamp	6 h	air	Ice bath	96	7
9	A-CTF-2	300 W Xe lamp (λ > 400 nm)	4h	O_2	RT	98	8
10	BP/CN	300 W Xe lamp (λ ≥ 420nm)	12h	O_2	25	99	9

References

1. Z. Shi, J. Li, Q. Han, X. Shi, C. Si, G. Niu, P. Ma and M. Li, *Inorg. Chem.*, 2019, **58**, 12529-12533.

2. J. He, Q. Han, J. Li, Z. Shi, X. Shi and J. Niu, *Journal of Catalysis*, 2019, **376**, 161-167.

3. Q. Li, J. Wang, Y. Zhang, L. Ricardez-Sandoval, G. Bai and X. Lan, *ACS Appl. Mater. Interfaces*, 2021, **13**, 39291-39303.

4. K. Jaiswal, Y. R. Girish and M. De, *ACS Appl. Nano Mater.*, 2020, **3**, 84-93.

5. R. Garg, S. Mondal, L. Sahoo, C. P. Vinod and U. K. Gautam, *ACS Appl. Mater. Interfaces*, 2020, **12**, 29324-29334.

6. H. Li, Y. Yang, C. He, L. Zeng and C. Duan, *ACS Catal.*, 2019, **9**, 422-430.

7. Y. Zhou and J. Long, *Optical Materials*, 2020, **109**, 110432.

8. X. Lan, X. Liu, Y. Zhang, Q. Li, J. Wang, Q. Zhang and G. Bai, *ACS Catal.*, 2021, **11**, 7429-7441.

9. Y. Li, H. Wang, X. Zhang, S. Wang, S. Jin, X. Xu, W. Liu, Z. Zhao and Y. Xie, *Angew. Chem., Int. Ed.*, 2021, **60**, 12891-12896.